Molecular Pharmacology Fast Forward. Published on February 11, 2021 as DOI: 10.1124/molpharm.120.000217
This article has not been copyedited and formatted. The final version may differ from this version.

Elevated cAMP protects against diclofenac-induced toxicity in primary rat hepatocytes: a protective effect mediated by EPACs

Fabio Alejandro Aguilar Mora*, Nshunge Musheshe*, Asmaa Oun, Manon Buist-Homan, Frank Lezoualc'h, Xiaodong Cheng, Martina Schmidt**, Han Moshage**

*: Authors contributed equally to this study

**: Authors contributed equally to this study

FAAM, MB-H, HM: Dept. Gastroenterology and Hepatology, University Medical Center Groningen, University of Groningen, Groningen, Netherlands

FL: Inserm UMR-1048, Institut des Maladies Métaboliques et Cardiovasculaires, Univ Toulouse Paul Sabatier, Toulouse, France

XC: Department of Integrative Biology & Pharmacology, Texas Therapeutics Institute, University of Texas Health Science Center at Houston, Houston, US

NM, AO, MS: Dept. Molecular Pharmacology, Groningen Research Institute of Pharmacy, Groningen Research Institute for Asthma and COPD, GRIAC, University Medical Center Groningen, University of Groningen, Groningen, Netherlands

MB-H, HM: Dept. Laboratory Medicine, University Medical Center Groningen, University of Groningen, Groningen, Netherlands

Molecular Pharmacology Fast Forward. Published on February 11, 2021 as DOI: 10.1124/molpharm.120.000217
This article has not been copyedited and formatted. The final version may differ from this version.

A. **Author information**

Fabio Alejandro Aguilar Mora
f.a.aguilar.mora@umcg.nl

Nshunge Musheshe
n.musheshe@rug.nl

Asmaa Oun
a.oun@rug.nl

Manon Buist-Homan
m.buist-homan@umcg.nl

Frank Lezoualc'h
Frank.Lezoualch@inserm.fr

Xiaodong Cheng
Xiaodong.Cheng@uth.tmc.edu

Martina Schmidt
m.schmidt@rug.nl

Han Moshage
a.j.moshage@umcg.nl

B. **Running title**: cAMP protects against diclofenac-induced toxicity via EPAC

C. **Corresponding Author**

Han Moshage
Postal address; University Medical Centre Groningen, Dept.
Gastroenterology and Hepatology Groningen,
NL 9713 GZ;
Netherlands
a.j.moshage@umcg.nl
Telephone; +31 50 361 2364

D. **Number of figures 10**
E. **Number of tables 0**
F. **Number of text pages 39**
G. **Number of references 58**
H. **Number of words in the abstract 250**
I. **Number of words in the introduction 845**
J. **Number of words in the discussion 1808**

Molecular Pharmacology Fast Forward. Published on February 11, 2021 as DOI: 10.1124/molpharm.120.000217
This article has not been copyedited and formatted. The final version may differ from this version.

K. **Number of tables to print 0**

L. Chemical compounds

a. Diclofenac sodium (PubChem CID;5018304)
b. IBMX (PubChem CID; 3758)
c. Forskolin (PubChem CID; 47936)
d. Rp-8-CPT-cAMP (PubChem CID; 23679060)
e. CE3F4 (PubChem CID; 21781066)
f. ESI-O5 (PubChem CID; 272513)

M. List of abbreviations and definitions in alphabetical order

AC: adenylyl cyclase

ADR: adverse drug reaction

AoD: Assay-on-Demand

ATP: adenosine triphosphate

AUF: arbitrary units of fluorescence

cAMP: cyclic adenosine monophosphate

CNG: cyclic nucleotide-gated

CTCF: corrected total cell fluorescence

DF: diclofenac

DILI: drug-induced liver injury

DISC: death-inducing signaling complex

DMEM: Dulbecco's Modified Eagle's medium

ECL; Enhanced chemiluminescence

EDTA: Ethylenediaminetetraacetic acid

EPAC: Exchange Protein Directly Activated by cAMP/cAMP-regulated guanine nucleotide exchange factors

EPAC1-HA: heme-agglutinin-tagged EPAC1

FIC: fold induction *vs* control

Forskolin: 7β-Acetoxy-8,13-epoxy-1α,6β,9α-trihydroxylabd-14-en-11-one

GSH: glutathione

GSSG: glutathione disulfide

HEPES: 4-(2-hydroxyethyl)-1-piperazineethanesulfonic acid

HEK 293: Human Embryonic Kidney 293 cell line

H_2O_2: hydrogen peroxide

Molecular Pharmacology Fast Forward. Published on February 11, 2021 as DOI: 10.1124/molpharm.120.000217
This article has not been copyedited and formatted. The final version may differ from this version.

JNK: c-Jun N-terminal kinase

PKA: protein kinase A

MGV: mean gray value

Mito: mitochondrial fraction

MMP: mitochondrial membrane potential

MPTP: permeability transition pore

NSAID: non-steroidal anti-inflammatory drug

OXPHOS: oxidative phosphorylation

PCC: pump-controlled cell rupture system

PDE: phosphodiesterase

PGE2: prostaglandin E2

Popdc proteins: Popeye domain

P13-K: phosphoinositide-3-kinase

RCF: relative centrifugal force

RIPA buffer: radioimmunoprecipitation assay buffer

p-VASP: vasodilator stimulated phospho-protein

RP: RP-8CPT-cAMPS

sAC: soluble adenylyl cyclase

SDS-PAGE: sodium dodecyl sulfate-polyacrylamide gel electrophoresis

TBS: Tris-buffered saline

Tim23: mitochondrial protein import complex

TNF-α: tumor necrosis factor-alpha

WCL: whole cell lysate

4-OH: 4’-hydroxydiclofenac

5-OH: 5’-hydroxydiclofenac

Molecular Pharmacology Fast Forward. Published on February 11, 2021 as DOI: 10.1124/molpharm.120.000217
This article has not been copyedited and formatted. The final version may differ from this version.

Abstract

Background: Chronic consumption of the nonsteroidal anti-inflammatory drug diclofenac may induce drug-induced liver injury (DILI). The mechanism of diclofenac-induced liver injury is partially elucidated and involves mitochondrial damage. Elevated cAMP protects hepatocytes against bile acid-induced injury. However, it is unknown whether cAMP protects against DILI and, if so, which downstream targets of cAMP are implicated in the protective mechanism including the classical protein kinase A (PKA) pathway or alternative pathways like the exchange protein directly activated by cAMP (EPAC). **Aim:** Investigate whether cAMP and/or its downstream targets protect against diclofenac-induced injury in hepatocytes. **Methods:** Rat hepatocytes were exposed to 400 µmol/L diclofenac. Apoptosis and necrosis were measured by caspase-3 activity assay and Sytox green staining respectively. Mitochondrial membrane potential (MMP) was measured by JC-10 staining. mRNA and protein expression were assessed by qPCR and Western blot, respectively. The cAMP-elevating agent forskolin, the pan-phosphodiesterase inhibitor IBMX and EPAC inhibitors CE3F4 and ESI-O5 were used to assess the role of cAMP and its effectors, PKA or EPAC. **Results:** Diclofenac exposure induced apoptotic cell death and loss of MMP in hepatocytes. Both forskolin and IBMX prevented diclofenac-induced apoptosis. EPAC inhibition, but not PKA inhibition abolished the protective effect of forskolin and IBMX. Forskolin and IBMX preserved the MMP while both EPAC inhibitors diminished this effect. Both EPAC1 and EPAC2 were expressed in hepatocytes and localized in mitochondria. **Conclusion:** cAMP elevation protects hepatocytes against diclofenac-induced cell death, a process primarily involving EPACs. The cAMP/EPAC pathway may be a novel target for treatment of DILI.

Keywords: cAMP, diclofenac, hepatocyte, apoptosis, EPAC, protein kinase A, mitochondria

Molecular Pharmacology Fast Forward. Published on February 11, 2021 as DOI: 10.1124/molpharm.120.000217
This article has not been copyedited and formatted. The final version may differ from this version.

Significance Statement

Our study shows two main highlights. First, elevated cAMP levels protect against diclofenac-induced apoptosis in primary hepatocytes via maintenance of mitochondrial integrity. In addition, we propose the existence of mitochondrial cAMP-EPAC microdomains in rat hepatocytes, opening new avenues for targeted therapy in DILI. Both EPAC1 and EPAC2, but not PKA, are responsible for this protective effect. Our findings present cAMP-EPAC as a potential target for the treatment of drug-induced liver injury (DILI) and liver injury involving mitochondrial dysfunction.

1 Introduction

Diclofenac is an over-the-counter non-steroidal anti-inflammatory drug (NSAID) with anti-inflammatory, anti-pyretic and analgesic properties. Diclofenac inhibits eicosanoid synthesis, in particular prostaglandin E_2 (PGE_2) and thromboxane via inhibition of both isoforms, COX-1 and COX-2, of the eicosanoid synthesizing enzyme cyclooxygenase, with selectivity towards COX-2 (Gan, 2010).

Although diclofenac is a well-tolerated drug, consumption of diclofenac can induce drug-induced liver injury (DILI). 6-18 cases per 100,000 persons/year develop severe hepatic adverse drug reactions (ADR) caused by the consumption of diclofenac (Boelsterli, 2003), with said numbers predicted to be underestimated due to underreporting - numbers expected to be 10-20 fold higher. It has been reported that diclofenac consumption at a dose of 200 mg/day for 30 days is the third-highest risk for ADRs in comparison to other NSAIDs (Lapeyre-Mestre, Grolleau and Montastruc, 2013). Due to the delayed onset of disease related patient-specific parameters such as poor drug metabolism, low metabolite clearance

and enterohepatic circulation rate (Seitz and Boelsterli, 1998), diclofenac-induced liver injury is impossible to diagnose before the irreversible stage thereby making it difficult to treat (Boelsterli, 2003; Aithal and Day, 2007).

Diclofenac metabolism in the liver has been comprehensively discussed previously (Aithal and Day, 2007). In brief, the first toxic diclofenac metabolites 4'-hydroxydiclofenac (4-OH) and 5'-hydroxydiclofenac (5-OH) are derived from phase-I reactions catalyzed by CYP2C9, CYP3A4 and CYP2C8, respectively. Phase II metabolism of diclofenac involves glucuronidation by the enzyme UGT2B1 (in rats) or UGT2B7 (in humans) resulting in diclofenac 1-O-β-acyl glucuronide (Boelsterli, 2003). Formation of these toxic metabolites is believed to increase reactive oxygen species production, followed by the depletion of glutathione (GSH) and NAD(P)H. Furthermore, both 4-OH and 5-OH can induce mitochondrial damage by increasing the mitochondrial membrane permeability transition pore (MPTP), leading to the depolarization of the mitochondrial membrane and inhibition of ATP synthesis (Syed, Skonberg and Hansen, 2016; Wang *et al.*, 2016) and ultimately inducing apoptotic death of hepatocytes (Gan, 2010).

The second messenger 3',5'-cyclic adenosine monophosphate (cAMP) is synthesized by catalytic conversion of ATP by plasma membrane-bound adenylyl cyclase (pmAC) on hormonal activation of G_s coupled receptors and by Ca^{2+} and bicarbonate-sensitive soluble adenylyl cyclase (sAC) (Wiggins *et al.*, 2018; Rahman *et al.*, 2013). cAMP is degraded by phosphodiesterases (PDE) - a superfamily of enzymes comprised of over 100 isoforms, and the only enzymes that degrade cAMP, thereby dictating the local level of cAMP at various subcellular sites (Jakobsen, Lange and Bak, 2019; Maurice *et al.*, 2014). PDEs are highly expressed in the liver and are in part localized in various organelles including the mitochondria, with PDE1A, PDE2, PDE3B, PDE8A and PDE11A being the most prominent

isoforms in human and rat liver (Lakics, Karran and Boess, 2010; Azevedo *et al.*, 2014; Monterisi *et al.*, 2017).

Downstream targets of cAMP include protein kinase A (PKA), the exchange protein directly activated by cAMP/ cAMP-regulated guanine nucleotide exchange factors (EPAC) (Franco, Bortner and Cidlowski, 2006; Schippers *et al.*, 2017), cyclic nucleotide-gated (CNG) channels and the recently discovered proteins containing the transmembrane Popeye domain – Popdc- proteins (Insel *et al.*, 2012). There are two EPAC proteins, EPAC1 and EPAC2, and two different genes encode them: Rap guanine nucleotide exchange factor (RAPGEF)3 and RAPGEF4, respectively. EPAC1 and EPAC2 are guanine-nucleotide exchange factors for the Ras-like GTPases Rap1 and Rap2 (Hoivik *et al.*, 2013). However, EPAC1 is expressed abundantly in all tissues; little or no expression has been reported in rat hepatocytes (Hoivik *et al.*, 2013). EPAC2 expression is more restricted and tissue-specific. EPAC2 has three isoforms, EPAC2A, 2B and 2C, as a result of differential splicing and it is the principal EPAC expressed in the liver, with EPAC2C being the most abundant isoform in the liver (Hoivik *et al.*, 2013; Sivertsen Åsrud *et al.*, 2019). Recent evidence suggests that EPAC plays a major role in metabolic pathways previously thought to be controlled by PKA (Insel *et al.*, 2012). Indeed, evidence has shown that in addition to PKA, EPAC alters mitochondrial function in both brain cells and cardiomyocytes, thereby suggesting that EPAC, as a downstream target of cAMP, is a novel target for the treatment of neurological diseases and the prevention of cardiovascular ailments (Wang *et al.*, 2016; Jakobsen, Lange and Bak, 2019; Fazal L et al., 2017).

However, a role for the cAMP-EPAC pathway in hepatocytes has not been demonstrated to date. In the liver, elevated cAMP levels protect against endoplasmic reticulum stress caused by bile acids via activation of EPAC and phoshoinositide-3-kinase/Akt (PI3-K/Akt) and the subsequent inhibition of phosphorylation of the pro-apoptotic kinase c-jun NH_2-terminal

kinase (JNK). In addition, elevated cAMP levels prevent tumor necrosis factor-α (TNF-α)-induced apoptosis by inhibiting the death-inducing signaling complex (DISC) via a mechanism mediated by PKA (Cullen *et al.*, 2004; Gates *et al.*, 2009; Johnston *et al.*, 2011; Bhattacharjee *et al.*, 2012). Mitochondrial impairment is an important factor in diclofenac-induced hepatic toxicity; however, it is unknown whether regulation of cAMP levels prevents hepatic damage caused by diclofenac and, if so, whether EPAC is involved in this protection. The hypothesis, therefore, was that regulation of cAMP levels protects against diclofenac-induced injury in primary rat hepatocytes and that this protection is achieved via EPAC signaling.

2 Materials and Methods

2.1 Compliance with requirements for studies using animals

2.1.1 Validity

Wistar rats were chosen for this research due to the similarity of cytochrome P450 expression in comparison to human cells. Furthermore, the Wistar rat is an accepted experimental animal species for the study of drug-induced liver toxicity and the majority of literature available has been performed using (Wistar) rats and cells derived from this species (Bhakuni *et al.*, 2016). Also, cell lines such as the HepG2 hepatoma cell line do not express cytochrome P450 enzymes, which is crucial for the study of drug metabolism (Rodríguez-Antona *et al.*, 2002).

Molecular Pharmacology Fast Forward. Published on February 11, 2021 as DOI: 10.1124/molpharm.120.000217
This article has not been copyedited and formatted. The final version may differ from this version.

2.1.2 Ethical statement

All experiments were performed according to the Dutch law on the welfare of laboratory animals (The Animal act 2011) and the Permission No 16778-01-002 of the committee for care and use of laboratory animals of the University of Groningen.

2.1.3 Animals

Specified pathogen-free male Wistar rats (220-250 g) aged 5-8 weeks were purchased from Charles River Laboratories Inc (Wilmington, MA, USA). Rats were housed in polypropylene cages at room temperature (25 ± 2 ºC) with standard bedding, regular 12 hour light/dark cycle, free access to standard laboratory chow and water. Experiments were performed following the guidelines of the local Committee for Care of laboratory animals.

2.2 Rat hepatocyte isolation

Primary rat hepatocytes (Rat hepatocytes) were isolated from Wistar rats using the two-step collagenase perfusion method under anesthesia with isoflurane 5%, followed by 60 mg/kg ketamine (Alfasan, Netherlands BV) combined with 0.25 mg/kg medetomidine (Orion Pharma, Finland) as described previously (Moshage, Casini and Lieber, 1990). After isolation, hepatocyte viability was assessed using trypan blue exclusion assay and only hepatocyte isolations with viability of more than 85% were used and cultured in collagen-coated (PureCol® Advanced BioMatrix) plates in Williams E medium (Thermo Fisher Scientific, Waltham, MA, USA Cat N32551020) supplemented with 50 µg/mL gentamicin (Thermo Fisher Scientific), 50 nmol/L dexamethasone (Sigma-Aldrich, Zwijndrecht, the Netherlands) and 5% fetal calf serum (Thermo Fisher Scientific) and penicillin, streptomycin and fungizone (PSF) for 4 h at 37 ºC and 5% CO_2 to allow cell attachment.

Molecular Pharmacology Fast Forward. Published on February 11, 2021 as DOI: 10.1124/molpharm.120.000217
This article has not been copyedited and formatted. The final version may differ from this version.

2.3 Experimental design

Primary rat hepatocyte isolations were performed for each experiment (n=3) with each experimental condition performed in duplicate (n=6). Experiments started 4 hours after the attachment of the cells. As a model of DILI-induced toxicity we used diclofenac (2-[(2,6-Dichlorophenyl) amino] benzene acetic acid sodium salt). This model has been described and induces predominantly apoptotic cell death in primary rat hepatocytes (Gan, 2010; Santos-Alves *et al.*, 2014). The optimal concentration for the experiments was defined by performing a dose-response curve (200-900 µmol/L) and a time curve (0-24 hours) as shown in Supplementary Figure 1. The pan-phosphodiesterase inhibitor IBMX (3-isobutyl-1-methylxanthine) and the AC agonist forskolin (7β-acetoxy-8,13-epoxy-1α,6β,9α-trihydroxylabd-14-en-11-one) (Merck®, Germany) were used to elevate cAMP levels and added 30 min before diclofenac. The optimal concentration of forskolin was determined by performing a dose-response curve (5-50 µmol/L) (Supplementary Figure 2), whereas IBMX was used at 100 µmol/L, which is the concentration most commonly used in the literature. IBMX and forskolin were subsequently used at 100 µmol/L and 10 µmol/L, respectively. The PKA inhibitor Rp-8-CPT cAMP (8-[(4-chlorophenyl)thio]-adenosine cyclic 3',5'-[hydrogen (R)-phosphorothioate]) (Cayman Chemicals®, USA) was used at 100 µmol/L as described previously (Gjertsen *et al.*, 1995; Hong, Zhang and Harbrecht, 2010; Schmidt, Dekker and Maarsingh, 2013). CE3F4 (5,7-dibromo-6-fluoro-3,4-dihydro-2-methyl-1(2H)-quinoline carboxaldehyde) was used as EPAC-1 inhibitor at 10 µmol/L and ESI-O5 (1,3,5-Trimethyl-2-[(4-methylphenyl) sulfonyl]-benzene, mesityl (4-methylphenyl) sulfone) was used as EPAC-2 inhibitor at 15 µmol/L. Before the start of the experiments, fresh Williams E medium (Thermo Fisher Scientific, Waltham, MA, USA Cat N32551020) without fetal calf serum and supplemented with 50 µg/mL gentamycin (Thermo Fisher Scientific), 50 µmol/L dexamethasone (Sigma-Aldrich, Zwijndrecht, the Netherlands) and PSF was added. Samples

were randomly labeled to avoid group or treatment identification until after the analysis was completed. All the results presented in this research represent *in vitro* experiments using primary rat hepatocytes (rat hepatocytes).

2.4 Cell culture and transfection

Human Embryonic Kidney 293 (HEK 293) cells were maintained in Dulbecco's Modified Eagle's medium (DMEM, Gibco™, 1960044) supplemented with 10% FBS and 1% penicillin-streptomycin-glutamine (Gibco™, 10378016). Briefly, HEK 293 cells were seeded overnight in 6-well plates at a seeding density of 500,000 cells/well. HEK 293 cells were transfected with 3 µg DNA constructs of either human EPAC2A, human EPAC2B, or HA-tagged EPAC1 (EPAC1-HA) (Laudette *et al.*, 2019) by using JetPEI® DNA Transfection Reagent (PolyPlus; cat. # 101-40N) according to the manufacturer's protocol. 3 µg of DNA were diluted first in 150 mmol/L NaCl. Diluted DNA was gently vortexed. JetPEI reagent was diluted in 150 mmol/L NaCl and gently vortexed. The JetPEI solution was then added to the DNA solution and incubated for 15 minutes at room temperature. The DNA/JetPEImix was added drop-wise to the HEK 293 cells. 48 hours after transfection, the cells were washed with ice-cold PBS and then lysed using a lysis buffer (0.25 mol/L), D-Mannitol (Fluka), 0.05 mol/L Tris-Base (Sigma), 1 mmol/L EDTA (Sigma #E6758), 1 mmol/L EGTA (Sigma #E4378) up to the required volume in water. pH was adjusted to 7.8. Before use, the lysis buffer was complemented with 1% Triton-X-100, 1% of 100 mmol/L dithiothreitol (DTT) and in addition supplemented with protease and phosphatase inhibitors. The lysate was spun down at 12,000 rcf (relative centrifugal force) at 4°C for 20 min and the supernatant was kept. Protein concentration was determined using the Pierce™ BCA Protein Assay Kit (Pierce™ BCA Protein Assay Kit, Thermo Scientific, Rockford, USA, #23225). For optimal

visualization of protein expression using ECL, membranes were exposed for either a short or a long time as appropriate**.**

2.5 Isolation of mitochondria

Freshly isolated primary rat hepatocytes mitochondria were isolated employing a semi-automated pump-controlled cell rupture system (PCC) (speed 0.71 ml/minutes) and syringes (SGE, Trajan© Scientific, Australia) attached to a cell homogenizer (Isobiotech, EMBL Heidelberg, Germany) superimposed on a pump (ProSense, Oosterhout, NL, #NE-1000) as described (Honrath *et al.*, 2017). Mitochondria were suspended in mitochondria isolation buffer (sucrose 250 mmol/L, 4-(2-hydroxyethyl)-1-piperazineethanesulfonic acid (HEPES), 20 mmol/L and Ethylenediaminetetraacetic acid (EDTA) 3 mmol/L adjusted to pH 7.2 (the entire procedure was performed on ice). The amount of protein derived from the isolation procedure was determined using the Pierce™ BCA Protein Assay Kit (Pierce™ BCA Protein Assay Kit, Thermo Scientific, Rockford, USA, #23225).

2.6 Western blotting

Cultured primary rat hepatocytes were lysed with a modified Radioimmunoprecipitation assay buffer (RIPA buffer) (50 mmol/L Tris-base, pH 7.4, 0.2% Triton X-100, 0.25 % Na-deoxycholate, 150 mmol/L NaCl, 1 mmol/L EDTA) supplemented with protease and phosphatase inhibitors. Pellets were clarified by centrifugation at 12000 rcf for 20 minutes at 4 °C. Protein concentration was determined using the BCA assay (Pierce™ BCA Protein Assay Kit, Thermo Scientific, Rockford, USA, #23225). Either 5 µg of HEK 293 cells overexpressing EPAC1-HA, EPAC2A or EPAC2B, 40 µg of protein (whole cell lysate) or 80

µg of total, cytosolic and mitochondria samples were separated by sodium dodecyl sulfate-polyacrylamide gel electrophoresis (SDS-PAGE). 10% or 12% gels were used (Resolving gel: 30% Acrylamide/BIS solution 40% w/v (Serva GmbH Germany, #10680.01), 1.5M Tris pH 8.8, 10% SDS, 10% ammonium persulfate, 0.04% Tetramethylethylenediamine (TEMED) all in distilled water; stacking gel: 30% acrylamide mix, 1.0 M Tris pH 6.8, 10% SDS, 10% ammonium persulfate, 0.1% TEMED, all up to a required volume in distilled water and subsequently transferred to nitrocellulose membranes (GE Healthcare, Amersham TM Protran TM, 0.45 µm NC #10600002). Membranes were blocked in 2.5% skim milk for 30 minutes and then incubated at 4ºC overnight in the following primary antibodies in 1% skim milk as appropriate: EPAC1 (Cell Signaling Technology, 5D3 #4155S (1:1000), EPAC2 (Cell Signaling Technology, 5B1 #4156S (1:1000), β-Actin (Sigma, A5441 #127M4866V (1:3000), Mitochondrial protein import complex (Tim23) (BD Bioscience, #127M4866V (1:1000), Vasodilator stimulated phospho-protein (p-VASP) (Cell Signaling Technology®, #3112 (1:100)). After at least 5 washes with Tris-buffered saline (TBS) with 1% Tween, membranes were incubated at room temperature for 1 hr in anti-mouse IgG-peroxidase produced in rabbit (Sigma, #029M4799V (1:3000) secondary antibody. Enhanced chemiluminescence (ECL) detection kit was used for the detection of protein expression on the membrane (PerkinElmer Inc, Waltham, USA, #NEL103E001EA).

2.7 Immunofluorescence

Immunofluorescence microscopy was performed on rat hepatocytes (4.5×10^5) on glass coverslips in 12-well plates. Monoclonal antibodies against EPAC1 and EPAC2 (Cell Signaling Technology®, catalog number #4155 and # 43239, respectively) were used at a dilution of 1:200 in 1% BSA/PBS 1X at room temperature for 1 hour. Images were captured on a Leica CTR 600 FS fluorescence microscope (Leica Microsystems, Amsterdam, the

Netherlands) at excitation/emission wavelengths of 460-500/512-542 nm, respectively with a 63X objective and at least three areas were randomly assessed using the LAS X software (Leica). The results for the reported research represent at least three independent hepatocyte isolations (n=3).

2.8 RNA isolation and quantitative real-time reverse transcription-polymerase chain reaction (qRT-PCR)

At the end of the experiments, cells were washed with ice-cold PBS and total RNA was isolated with TRI-reagent (Sigma-Aldrich, St Louis, MO) according to the manufacturer's instructions. Reverse transcription (RT) was performed using 2.5 µg of total RNA, 1X RT buffer (500 mmol/L Tris-HCL [pH8.3]; 500 mmol/l KCl; 30 mmol/l $MgCl_2$; 50 mmol/l DTT), 10 mmol/l deoxynucleotides triphosphate (dNTPs, Sigma-Aldrich, St-Louis, MO), 10 ng/µl random nanomers (Sigma Aldrich, St Louis, MO), 0.6 U/µl RNaseOUT™ (Invitrogen, Carlsbad, CA) and 4 U/µl M-MLV reverse transcriptase (Invitrogen, Carlsbad, CA) in a final volume of 50 µl. The cDNA synthesis program was 25°C/10 min, 37°C/60 min and 95°C/5 min. Complementary DNA (cDNA) was diluted 20× in nuclease-free water. Real-time qPCR was carried out in a QuantStudio 3™ (96-well) PCR System (Applied Biosystems, ThermoFisher, Wilmington, DE). The assessment of universal RAPGEF3 and universal RAPGEF4 was determined using an Assay-on-Demand (AoD) TaqMan® (Thermo Fisher Scientific, Sunol Blvd, Pleasanton, CA) (rat probe EPAC1/RAPGEF3: catalog number Rn00572463_m1 and rat probe EPAC2/RAPGEF4: catalog number Rn01514839_m1. The assessment of RAPGEF 4 isoforms (RAPGEF4A, RAPGEF4B and RAPGEF4C) was determined using SYBR Green according to the primer sets described previously (Hoivik *et al.*, 2013; Sivertsen Åsrud *et al.*, 2019). For the Assay-on-Demand (AoD) Taqman qPCR, 2× reaction buffer (dNTPs, Hot Gold Star DNA polymerase, 5 mmol/l $MgCl_2$) (Eurogentec,

Belgium, Seraing) and 20x AoD gene expression assay mix were used. For the SYBR-Green the fast Start Universal SYBR Green Master (ROX) (Roche 0413914001) was used. Both assays used 50 µmol/L of sense and antisense primers (Invitrogen). mRNA levels were normalized to the 18S housekeeping gene and subsequently normalized to the mean expression level of the control group. Samples represent at least three independent hepatocyte isolations (n=3). The primer sequences can be found in Supplementary Table 1.

2.9 Caspase 3 enzyme activity assay

Caspase-3 enzyme activity was assayed as described previously (Schoemaker *et al.*, 2002). Fluorescence was quantified using a spectrofluorometer at an excitation wavelength of 380 nm and an emission wavelength of 430 nm. The arbitrary units of fluorescence were normalized to the control and expressed as fold induction *vs* control to avoid an unwanted source of variation. The results for the reported research represent at least three independent hepatocyte isolations (n=3) with duplicated conditions. Mann-Whitney u test was used to determine statistical significance (n=6). All samples were included in the analysis and no post-hoc analysis was done.

2.10 Sytox green nuclear staining

Rupture of the plasma membrane distinguishes necrotic from apoptotic cell death. To estimate necrotic cell death hepatocytes were incubated for 15 min with Sytox green (ThermoFisher Scientific® ; Cat. nr: S7020) nucleic acid stain. Sytox green only penetrates necrotic cells with compromised plasma membrane but does not cross the membrane of viable cells or apoptotic bodies. Hepatocytes exposed to 5 mmol/L hydrogen peroxide (H_2O_2) for 24 hours were used as a positive control for necrosis (Conde de la Rosa *et al.*, 2006). Fluorescent nuclei were evaluated in three randomly selected areas from three independent

hepatocyte isolations for each condition and the images were captured on a Leica CTR 600 FS fluorescence microscope (Leica® Microsystems, Amsterdam, The Netherlands) using a 10X objective. Quantification of the necrotic cells was performed by the determination of the percentage of cell viability with the ImageJ software. By selecting 3-5 random areas of each image and counting the intact nuclei (non-stained) vs stained nuclei, a characteristic of necrotic cells (Conde de la Rosa *et al.*, 2006) to obtain the raw percentage of cell viability of selected conditions. The raw percentage of cell viability was then normalized to the average percentage of cell viability of the control condition (DMSO) (mean value was set to 100%) to prevent unwanted sources of variation. The percentage of cell viability vs control was used to describe the results. Mann-Whitney u test was used to determine differences between groups and statistical analysis was done with at least a group of n=8. All samples were included in the analysis and no posthoc analysis was performed. The information is shown as the median (interquartile- range). The quantification of Sytox green staining is depicted in Supplementary Table 2.

2.11 Mitochondrial membrane potential analysis (MMP)

Measurement of mitochondrial membrane potential was evaluated using the dye JC-10 (Enzo Life Sciences®, Farmingdale, NY, USA ENZ-52305). Red staining represents aggregates, indicating polarization of the mitochondrial membrane potential ($\Delta\psi m$) while green staining represents monomers, indicating depolarization. Since cells need to preserve an ion gradient across the membrane, to maintain the respiratory chain function, red staining indicates that the oxidation-reduction potential of the mitochondria is healthy (Franco, Bortner and Cidlowski, 2006). In contrast, upon cell injury, green monomers accumulate in the cells due to the opening of the mitochondrial permeability transition pore (MPTP), allowing passage of ions and small molecules, resulting in a disequilibrium of ions across the mitochondrial

Molecular Pharmacology Fast Forward. Published on February 11, 2021 as DOI: 10.1124/molpharm.120.000217
This article has not been copyedited and formatted. The final version may differ from this version.

membrane, resulting in the loss of charge (depolarization) and uncoupling of the respiratory chain. Cells were stained with 100 µmol/L JC-10 for 15–30 min 2 hours after exposure to diclofenac with its respective pretreatment (forskolin, IBMX or EPAC inhibitors). Three areas were randomly selected from at least three independent hepatocyte isolations for each condition and the images were obtained on a Leica CTR 600 FS fluorescence microscope (Leica® Microsystems,) using a 10X objective. Quantification of the fluorescence intensity and the red/green ratio was calculated using ImageJ software. The quantification was performed by quantifying and comparing the integrated density (intDen) of the red and green channel and mean gray value (MGV) to obtain the corrected total cell fluorescence (CTCF). CTCF was normalized to the average CTCF of the control condition (set as red/green ratio of 1.0) to prevent unwanted sources of variation and expressed as fluorescence intensity ratio (red/green). Mann-Whitney u test was used to determine differences between groups and statistical analysis was done with at least a group of n=6.

2.12 ATP determination

Twenty-five thousand primary hepatocytes were seeded in an opaque-walled 96 well plate. Incubations with test substances were performed for 2 to 4 hours. After incubation, the culture medium was removed and 100 µl of fresh Williams E medium with 100 µmol/L of CellTiter-Glo®3D reagent (Promega®, France) was added to each well. Plates were protected from light and shaken at room temperature for 5 min to induce cell lysis. Samples were then incubated for an additional 10 min at room temperature and protected from light. Fluorescence was recorded using a fluorescence plate reader Synergy (BioTek Instruments®, Inc., USA). AUF was normalized to controls to avoid unwanted sources of variation and three independent experiments were used to depict the results. The results for the reported research represent at least three independent hepatocyte isolations (n=3) with triplicate

conditions to depict the results. Mann-Whitney u test was used to determine statistical significance (n=9).

Molecular Pharmacology Fast Forward. Published on February 11, 2021 as DOI: 10.1124/molpharm.120.000217
This article has not been copyedited and formatted. The final version may differ from this version.

2.13 Statistical Analysis

Normality test was done using the Shapiro-Wilk test. Due to the non-normal distribution of the samples, statistical significance was analyzed using a two-tailed Mann-Whitney u test to compare differences between two groups. Results are presented as mean ± standard deviation (mean ± SD) ns $p > 0.05$, * $p \leq 0.05$, **, $p \leq 0.01$, ***: $p \leq 0.001$, ****: $p \leq 0.0001$. Statistical analysis was performed using GraphPad Prism 7 (Graphpad Software, San Diego, CA, USA).

Molecular Pharmacology Fast Forward. Published on February 11, 2021 as DOI: 10.1124/molpharm.120.000217
This article has not been copyedited and formatted. The final version may differ from this version.

3 Results

3.1 Elevation of cAMP prevents diclofenac-induced caspase 3 activity

Diclofenac-induced caspase-3 activity peaked at 400 µmol/L and 12 hours without inducing extensive necrotic death in primary rat hepatocytes (Supplementary Figure 1 and Supplementary Table 2). To investigate whether elevation of cAMP protects against diclofenac-induced apoptosis, cells were pretreated for 30 min with forskolin or IBMX followed by diclofenac intoxication. Both cAMP elevating agents; the AC agonist forskolin as well as the phosphodiesterase inhibitor IBMX prevented diclofenac-induced caspase-3 activity in primary hepatocytes (Figure 1). These results demonstrated a protective role of cAMP against diclofenac-induced apoptosis. By using Sytox green nuclear staining, it was possible to rule out the possibility that forskolin and IBMX induce necrotic cell death, thereby indicating that cAMP prevents diclofenac-induced hepatotoxicity without switching the mode of cell death from apoptosis to necrosis (Supplementary Table 2).

3.2 Protein Kinase A inhibition does not abolish the protective effect of cAMP on diclofenac-induced caspase 3 activity

Previous studies suggested that the downstream effects of cAMP were mainly mediated by the activation of protein kinase A (PKA) (Wolfgang *et al*., 1996). However, it is not known whether PKA mediates the protective effect of cAMP in diclofenac-induced hepatocyte toxicity. To test this hypothesis, cells were incubated with diclofenac in the presence or absence of the PKA inhibitor RP-8CPT-cAMPS. Rp-8CPT-cAMPS was added 30 min before the addition of the cAMP elevating agents and 60 min before diclofenac exposure (Figure 2). Effect of RP-8CPT-cAMPS on PKA was further elucidated by Western blot analysis of the

classical PKA effector vasodilator-stimulated phospho-protein (p-VASP) to confirm its effectiveness in inhibiting PKA activity and thus phosphorylation (Supplementary Figure 3). The inhibition of PKA only slightly prevented the protective effect of forskolin against diclofenac-induced caspase-3 activity (Figure 2, panel A) and it did not decrease the protective effect of IBMX (Figure 2, panel B). The PKA inhibitor RP-8CPT-cAMPS alone did not increase the caspase-3 activity in comparison to the control condition, ruling out a possible toxic effect of RP-8CPT-cAMPS (Figure 2 A, B). These results suggest that the protective effect of cAMP against diclofenac-induced apoptosis is not mediated by PKA activation.

3.3 Inhibition of EPAC1 and EPAC2 abolishes the protective effect of cAMP on diclofenac-induced caspase 3 activity

Since PKA does not mediate the protective effect of cAMP, we hypothesized that EPAC which is described as an alternative downstream target of cAMP signaling is involved in the protective effect of cAMP against diclofenac-toxicity (Schmidt, Dekker and Maarsingh, 2013). The role of EPAC in the protective effect of cAMP was investigated. Cells were pre-treated with either the EPAC1-specific inhibitor CE3F4 or the EPAC2-specific inhibitor ESI-05 60 min before diclofenac and 30 min before cAMP elevating agents forskolin or IBMX treatment. Inhibition of EPAC1 (Figure 3 panel A) or EPAC2 (Figure 3 panel C) abolished the protective effect of forskolin against diclofenac-induced caspase-3 activation (DF + forskolin *vs*. DF + forskolin + CE3F4 inhibitor) and (DF + forskolin *vs*. DF + forskolin + ESI-05 inhibitor). Inhibition of EPAC2 (Figure 3 panel B) or EPAC1 (Figure 3 panel D) also abolished the protective effect of IBMX against diclofenac-induced caspase-3 activation ((DF + IBMX *vs*. DF + IBMX + ESI-05 inhibitor) and (DF + IBMX *vs*. DF + IBMX + CE3F4 inhibitor)). ESI-05 or CE3F4 alone did not increase caspase-3 activity ((ESI-05 *vs*. Control)

Molecular Pharmacology Fast Forward. Published on February 11, 2021 as DOI: 10.1124/molpharm.120.000217
This article has not been copyedited and formatted. The final version may differ from this version.

and (CE3F4 *vs*. Control)) ruling out a possible toxic effect of ESI-05 or CE3F4. These results suggest that the protective effect of cAMP is mediated by EPAC1 and EPAC2.

3.4 EPAC1 and EPAC2 isoforms are expressed in primary rat hepatocytes

To corroborate our findings obtained with the pharmacological inhibitors, EPAC expression in primary rat hepatocytes was evaluated. mRNA expression analysis revealed expression of EPAC1 in total rat liver. EPAC1 expression was highest in liver sinusoidal cells (LSECs), followed by stellate cells, hepatocytes and Kupffer cells (Figure 4 and Supplementary Figure 4). Immunofluorescence revealed a 'punctate-like' staining pattern for EPAC1, indicative of a specific organellar localization of EPAC1 whereas EPAC2 revealed a more 'uniform' staining pattern (Figure 5, panel A). Subsequent analysis by Western blot revealed localization of EPAC1 in mitochondria of hepatocytes (Figure 5, panel B). EPAC2 mRNA was clearly expressed in total rat liver and hepatocytes (Figure 4). Furthermore, using mouse primers specific for the EPAC2 isoforms, we demonstrated significant mRNA expression of both EPAC2B and EPAC2C in rat hepatocytes (Figure 4, Supplementary Figure 4). Overexpressed human origin EPAC2A and EPAC2B in HEK 293 cells were used as positive controls in Western blot analysis to confirm protein expression of EPAC2 isoforms in rat hepatocytes. We show that both EPAC2B and EPAC2C are expressed in whole cell primary rat hepatocytes as well as in mitochondria (Figure 5, panel C).

Molecular Pharmacology Fast Forward. Published on February 11, 2021 as DOI: 10.1124/molpharm.120.000217
This article has not been copyedited and formatted. The final version may differ from this version.

3.5 Elevation of cAMP does not protect against ATP depletion caused by diclofenac in primary rat hepatocytes

Previous studies indicated that diclofenac-induced toxicity is associated with mitochondrial damage and ATP depletion (Syed, Skonberg and Hansen, 2016). To investigate whether the protective effect of cAMP is linked to the restoration of ATP levels, cells were incubated with diclofenac in the presence or absence of forskolin or IBMX followed by diclofenac exposure. Diclofenac decreased cellular ATP levels by 55% compared to the control condition after 2 hours of intoxication and by 87% after 4 hours of diclofenac intoxication (Figure 6). Elevation of cAMP levels using forskolin or IBMX did not prevent the depletion of ATP caused by diclofenac at either 2 or 4 hours (Figure 6). These results suggest that the protective role of cAMP against diclofenac-induced apoptosis is not related to an early recovery of ATP production.

3.6 Elevation of cAMP prevents mitochondrial membrane potential (MMP) depolarization induced by diclofenac in primary hepatocytes: an effect mediated by EPAC

Diclofenac-induced toxicity has been associated with mitochondrial damage. In that regard, we investigated the effect of cAMP on mitochondrial integrity during diclofenac intoxication and its potential connection to EPAC. Cells were incubated with diclofenac with or without prior ESI-05 (EPAC2 inhibitor) addition or CE3F4 (EPAC1 inhibitor). The control condition's red/green ratio was set at 1.0, as described in Materials and Methods. Diclofenac decreased the MMP (red/green ratio 0.69) in comparison to the control condition (Figure 7). The mitochondrial membrane depolarization caused by diclofenac was prevented by forskolin and IBMX, restoring the MMP ratio to 0.95 and 0.99, respectively (Figure 7). However, forskolin's protective effect in the presence of EPAC1 inhibitor was statistically significant

Molecular Pharmacology Fast Forward. Published on February 11, 2021 as DOI: 10.1124/molpharm.120.000217
This article has not been copyedited and formatted. The final version may differ from this version.

(Figure 8), indicating that EPAC1 is to a limited extent involved in maintaining the protective effect of forskolin against the mitochondrial membrane depolarization induced by diclofenac. In contrast, the protective effect of IBMX on MMP was abolished in the presence of the EPAC2 inhibitor (red/green ratio 0.65) (DF + IBMX *vs*. DF + IBMX + ESI-05 inhibitor) as shown in Figure 8. The protective effect of IBMX on the MMP was not affected when EPAC1 was inhibited (DF + IBMX *vs* DF + IBMX + CE3F4 inhibitor) as shown in Figure 8. These results suggest that the protective effect of forskolin involves EPAC1 whereas the protective effect of IBMX is mainly dependent on EPAC2, overall suggesting that the protective effect of cAMP against diclofenac-induced toxicity is related to preserving the integrity of the mitochondria, possibly via compartmentalized signaling of cAMP.

Molecular Pharmacology Fast Forward. Published on February 11, 2021 as DOI: 10.1124/molpharm.120.000217
This article has not been copyedited and formatted. The final version may differ from this version.

4 Discussion

This study shows that early elevation of cAMP prevents diclofenac-induced apoptosis in primary rat hepatocytes, with the protective effect being mediated by the downstream cAMP effector EPAC rather than PKA. Moreover, for the first-time, evidence is provided for a protective role of EPAC on mitochondrial integrity and function in primary rat hepatocytes. Furthermore, expression of EPAC1 and EPAC2 (particularly EPAC2B and EPAC2C) at both the mRNA and protein level in primary rat hepatocytes was observed. Most importantly, both EPAC1 and EPAC2 were also observed in mitochondria for the first time.

cAMP is spatially and temporally regulated, with physiologically relevant signals being those constrained in nano-domains, thereby allowing for distinct responses to be propagated within the cell - this is known as compartmentalization of cAMP. Compartmentalization of cAMP by synthesis via ACs, by degradation by PDEs and targeting of cAMP effector proteins by A-kinase anchoring proteins (AKAPs), are thought to profoundly affect the net-outcome of cAMP effects (Monterisi *et al.*, 2017; Zuo *et al.*, 2019; Cattani-Cavalieri, Valença and Schmidt, 2020; Ercu *et al.*, 2020). In this regard, cAMP elevation has the potential to regulate both pro-apoptotic and anti-apoptotic signals (Insel *et al.*, 2012). Although this study's topic was not compartmentalization of cAMP generation or function, the observation of mitochondrial AC-cAMP-EPAC1 and PDE-cAMP-EPAC2 domains in rat hepatocytes offers avenues for therapeutic targeting of cAMP compartments, with a specific emphasis on mitochondria.

This study demonstrated that elevation of cAMP levels either by direct activation of AC with forskolin or by inhibiting phosphodiesterases (PDEs) with IBMX prevents diclofenac-induced apoptosis in primary rat hepatocytes. These results are supported by previous research (Sinclair *et al.*, 2008; Gates *et al.*, 2009; Chamulitrat *et al.*, 2013) in which increased levels of cAMP were protective against the apoptotic effect of various toxic stimuli in rodent

hepatocytes. cAMP increase resulted in protection against endoplasmic reticulum stress caused by bile acids and also in the protection against TNFα-induced apoptosis by inhibiting the Death-Inducing Signaling Complex (DISC) (Cullen *et al.*, 2004; Gates *et al.*, 2009; Johnston *et al.*, 2011; Bhattacharjee *et al.*, 2012).

A protective effect of elevated cAMP against diclofenac-induced toxicity has not been reported before. Initially, we hypothesized that the protective effect might be due to the prevention of diclofenac-induced ATP-depletion; however, the observed changes in ATP levels do not justify an essential role of ATP in preventing diclofenac-induced toxicity.

Both EPAC1 and EPAC2 proteins are expressed in the liver (Ueno et al., 2001; Sivertsen Åsrud et al., 2019) (Hoivik *et al.*, 2013; Sivertsen Åsrud *et al.*, 2019). It has been reported that only EPAC2 is expressed in hepatocytes, mainly the EPAC2C isoform. In our study, we confirm and extend these findings at both the mRNA and protein levels. However, in contrast to previous reports, we did observe EPAC1 expression in rat hepatocytes both at the protein and mRNA level. EPAC1 expression was even higher in liver sinusoidal endothelial cells.

Moreover, in primary rat hepatocytes, we observed that EPAC1 protein is also localized at the mitochondria, explaining the protective effect of EPAC1. It has been suggested that the EPAC2 inhibitor ESI-O5, which was used in our study, is specific for EPAC2A and 2B (Rehmann, 2013). If EPAC2A is low or absent in hepatocytes, this implies that the observed protective effects of EPAC2 can be attributed to EPAC2B which is also localized at the mitochondria. Another probable explanation is that under stress conditions such as DILI, EPAC2A expression may be induced due to changes in the methylation status of the gene (Gervin *et al.*, 2017; Fromenty, 2020).

Although the function of EPAC in the liver remains to be fully characterized, previous reports suggest that EPAC modulates liver inflammation and the proliferation of stellate cells

in the liver (Yang *et al.*, 2016; Schippers *et al.*, 2017). Our results demonstrate an additional role of EPAC in the liver. We show that a AC-cAMP-EPAC1 and a PDE-cAMP-EPAC2 domain play a role in maintaining the mitochondrial membrane potential during diclofenac-induced toxicity. Although the role of EPAC in the mitochondria has been described previously in neurons (Jakobsen, Lange and Bak, 2019), this is the first time we show similar results in primary rat hepatocytes. The exact mechanism for the protective effect of EPAC against diclofenac-induced toxicity remains to be elucidated. Previous research has shown that cAMP can protect against glycochenodeoxycholic acid (GCDCA)-induced apoptotic death of hepatocytes, via a mechanism that involves EPAC inhibiting the phosphorylation of the pro-apoptotic kinase c-jun NH2-terminal kinase (JNK) (Gates *et al.*, 2009). Another mechanism that may explain the protective effect of EPAC was proposed by Szanda et al (Szanda et al., 2018). Szanda *et al* proposed that EPAC, more specifically EPAC1, regulates the MMP in isolated cortex mitochondria, via downstream effects on inositol trisphosphate receptors and Ca^{2+} channels. Ca^{2+} fluxes are known to affect mitochondrial functions such as MMP, antioxidant status, and, possibly, the OXPHOS pathway (Acin-Perez *et al.*, 2009). Besides, it has been shown that the activation of EPAC2-Rap1 can attenuate mitochondrial ROS production in myocardial cells (Yang *et al.*, 2017). Taken together, this suggests that the cAMP/EPAC pathway described in this paper may attenuate oxidative stress via the preservation of Ca^{2+} homeostasis.

In addition to the MMP, ATP production is an essential marker for mitochondrial integrity and function. Diclofenac-induced cytotoxicity is characterized by ATP depletion in a time-dependent manner (Sanuki *et al.*, 2017). Our results suggest that diclofenac induces ATP depletion as previously described; however, cAMP elevation does not protect against diclofenac-induced ATP depletion. A probable explanation might be that we use a relatively toxic (lethal) dose of 400 µmol/L diclofenac in which the ATP depletion is too extensive to

be compensated significantly by elevated cAMP levels. It is important to note that it is difficult to compare *in vitro* experimental conditions to plasma levels. Also, the dose we used was within the range previously reported in the literature for *in vitro* studies and it was found to be the minimal toxic dose (Boelsterli, 2003).

In our studies, we used the fluorescent dye JC-10 to determine the MMP. The use of cationic dyes, in particular JC-1, may have some drawbacks such as incorrect changes in fluorescence due to changes in the pH of medium or cells, Ca^{2+} release by the mitochondria and by the endoplasmic reticulum, and low solubility in water (Perry *et al.*, 2011). Of note, however, is that JC-10 dye was used, which has two important advantages over JC-1 such as; better water solubility and the ability to reverse its color from green to red/orange as the mitochondria become more polarized, thereby ensuring more consistent results. Furthermore, we have previously shown a strong correlation between the results obtained using the JC-10 probe and TMRE flow cytometry (Geng *et al.*, 2020). Therefore, we are confident that our MMP read-outs based on JC-10 are reliable.

Previous studies have demonstrated the importance of cAMP in mitochondrial function. cAMP modulates the activity of complex I via PKA-mediated phosphorylation of the 18kDa (AQDQ) subunit of complex I (Papa *et al.*, 1999) and the coupling efficiency and structural organization of the F_OF_1 subunits of complex V (ATP synthase), both of which are instrumental in the oxidative phosphorylation system (OXPHOS) (De Rasmo *et al.*, 2016). Although the effects of diclofenac on OXPHOS have not been fully characterized in the liver yet, a study in kidney cells suggests that diclofenac decreases the function of complex I (Ng *et al.*, 2006).

Our results are in line with a protective function of elevated cAMP levels. This is the first time EPAC has been identified as the downstream target of cAMP that is responsible for the protective effect against DILI in primary rat hepatocytes.

Sub-cellular cAMP's existence could explain the opposing effect of forskolin and IBMX results compartmentalized signaling (Monterisi *et al.*, 2017; Zuo *et al.*, 2019; Cattani-Cavalieri, Valença and Schmidt, 2020). For example, the mitochondrial matrix has been identified as containing a unique cellular cAMP compartment where sACs regulate cAMP and thus mitochondria function independently of the cytoplasm (Jakobsen, Lange and Bak, 2019) (Figure 10). In our current study, we focused on plasma-membrane bound AC (pmAC) activated by forskolin. The potential involvement of sAC remains to be studied. Subcellular cAMP compartments are also maintained by PDE isoforms (Monterisi *et al.*, 2017; Dawei *et al.*, 2019); however, a mitochondrial PDE-cAMP-EPAC2 domain is yet to be described. The compartmentalization of cAMP could explain the protection against depolarization of the MMP and ATP depletion and also suggests that mitochondrial ROS formation mainly occurs at complexes I and III and that cAMP effectors have no direct interaction with these complexes (Szanda *et al.*, 2018). In this regard, it remains to be elucidated how ACs may modulate ROS levels in mitochondria via modulation of OXPHOS. One possibility is that complex IV hyperphosphorylation can result in increased ROS generation in mitochondria (Valsecchi, Konrad and Manfredi, 2014). Another possibility is that excessive mitochondrial Ca^{2+} induces the mitochondrial permeability transition, which leads to cell death - this has been connected to diclofenac toxicity in previous studies (Masubuchi, 2002). In cardiomyocytes, it has been reported that activation of mitochondrial EPAC1 protects against overflow of the mitochondrial permeability transition by preventing Ca^{2+} overload via modulation of the mitochondrial calcium uniporter (Wang *et al.*, 2016). The exact role of both EPAC1 and EPAC2 in maintaining the balance of ROS in mitochondria requires further

Molecular Pharmacology Fast Forward. Published on February 11, 2021 as DOI: 10.1124/molpharm.120.000217
This article has not been copyedited and formatted. The final version may differ from this version.

characterization but certainly opens a new avenue for targeted drug therapy in DILI with a special focus on mitochondria.

It is worth discussing the specificity and potential off-target effects of the EPAC inhibitors in this study. CE3F4 primarily inhibits EPAC1 by binding to the catalytic domain of EPAC cyclic nucleotide-binding (CNB) domain (Courilleau *et al.*, 2013). Thus, CE3F4 most likely acts on the EPAC1 expressed in the primary hepatocytes and localized predominantly in mitochondria, explaining the inhibitory effect of CE3F4 on the protective effect of elevated cAMP. ESI-O5 is an inhibitor of EPAC2 isoforms A and B but not EPAC2C as it lacks the N-terminal CNB and DEP domain (Rehmann, 2013). As in our studies, EPAC2A was barely detectable; the observed protective effects of EPAC2 inhibition can be primarily attributed to EPAC2B, which is also localized at the mitochondria. Another explanation may be that under stress conditions such as DILI, EPAC2A expression may be induced due to changes in the methylation status of the gene (Gervin *et al.*, 2017; Fromenty, 2020). Further studies on the differential expression and subsequent impact of EPAC proteins on functional responses in primary rat hepatocytes will be fascinating but are beyond the current manuscript's scope.

In conclusion, in this study, we demonstrate cAMP's protective role against diclofenac-induced apoptosis in primary hepatocytes. Also, we report that EPAC proteins and not PKA is responsible for the protective mechanism. Both EPAC1 and EPAC2B and EPAC2C are expressed in primary rat hepatocytes. The mitochondrial localization of EPAC1 and EPAC2 suggests mitochondrial cAMP-EPAC domains, opening novel avenues in the targeted treatment of DILI.

Acknowledgments: The authors would like to thank Melissa van der Veen for excellent technical support and Augustin Boisleux to support the artwork.

Molecular Pharmacology Fast Forward. Published on February 11, 2021 as DOI: 10.1124/molpharm.120.000217
This article has not been copyedited and formatted. The final version may differ from this version.

Author contribution

Participated in research design: Mora, Musheshe, Schmidt and Moshage.

Conducted experiments: Mora, Musheshe, Buist-Homan and Oun.

Contributed new reagents or analytic tools: Oun, Buist-Homan, Lezoualc'h and Cheng.

Performed data analysis: Mora, Musheshe, Schmidt and Moshage.

Wrote or contributed to the writing of the manuscript: Mora, Musheshe, Buist-Homan, Schmidt and Moshage.

4 References

Acin-Perez, R. *et al.* (2009) 'Cyclic AMP produced inside mitochondria regulates oxidative phosphorylation.', *Cell metabolism*. NIH Public Access, 9(3), pp. 265–76. doi: 10.1016/j.cmet.2009.01.012.

Aithal, G. P. and Day, C. P. (2007) 'Nonsteroidal Anti-Inflammatory Drug-Induced Hepatotoxicity', *Clinics in Liver Disease*. Clin Liver Dis, pp. 563–575. doi: 10.1016/j.cld.2007.06.004.

Arnaiz, S. L. *et al.* (1995) 'Oxidative stress by acute acetaminophen administration in mouse liver', *Free Radical Biology and Medicine*. Pergamon, 19(3), pp. 303–310. doi: 10.1016/0891-5849(95)00023-Q.

Azevedo, M. F. *et al.* (2014) 'Clinical and molecular genetics of the phosphodiesterases (pdes)', *Endocrine Reviews*. Endocrine Society, 35(2), pp. 195–233. doi: 10.1210/er.2013-1053.

Bhakuni, G. S. *et al.* (2016) 'Animal models of hepatotoxicity', *Inflammation Research*, 65(1), pp. 13–24. doi: 10.1007/s00011-015-0883-0.

Bhattacharjee, R. *et al.* (2012) 'cAMP prevents TNF-induced apoptosis through inhibiting DISC complex formation in rat hepatocytes.', *Biochemical and biophysical research communications*. NIH Public Access, 423(1), pp. 85–90. doi: 10.1016/j.bbrc.2012.05.087.

Boelsterli, U. A. (2003) 'Diclofenac-induced liver injury: a paradigm of idiosyncratic drug toxicity', *Toxicology and Applied Pharmacology*. Academic Press, 192(3), pp. 307–322. doi: 10.1016/S0041-008X(03)00368-5.

Cattani-Cavalieri, I., Valença, S. dos S. and Schmidt, M. (2020) 'Nanodomains in cardiopulmonary disorders and the impact of air pollution', *Biochemical Society Transactions*. Portland Press, 48(3), pp. 799–811. doi: 10.1042/BST20190250.

Chamulitrat, W. *et al.* (2013) 'Ursodeoxycholyl Lysophosphatidylethanolamide Inhibits Lipoapoptosis by Shifting Fatty Acid Pools toward Monosaturated and Polyunsaturated Fatty Acids in Mouse Hepatocytes', *Molecular Pharmacology*, 84(5), pp. 696–709. doi: 10.1124/mol.113.088039.

Conde de la Rosa, L. *et al.* (2006) 'Superoxide anions and hydrogen peroxide induce hepatocyte death by different mechanisms: Involvement of JNK and ERK MAP kinases',

Journal of Hepatology. Elsevier, 44(5), pp. 918–929. doi: 10.1016/J.JHEP.2005.07.034.

Courilleau, D. *et al.* (2013) 'The (R)-enantiomer of CE3F4 is a preferential inhibitor of human exchange protein directly activated by cyclic AMP isoform 1 (Epac1)', *Biochemical and Biophysical Research Communications*. Academic Press Inc., 440(3), pp. 443–448. doi: 10.1016/j.bbrc.2013.09.107.

Cullen, K. A. *et al.* (2004) 'Activation of cAMP-guanine exchange factor confers PKA-independent protection from hepatocyte apoptosis.', *American journal of physiology. Gastrointestinal and liver physiology*, 287(2), pp. G334-43. doi: 10.1152/ajpgi.00517.2003.

Dawei, L. *et al.* (2019) 'PDE2 regulates membrane potential, respiration and permeability transition of rodent subsarcolemmal cardiac mitochondria', *Mitochondrion*. Elsevier B.V., 47, pp. 64–75. doi: 10.1016/j.mito.2019.05.002.

De Rasmo, D. *et al.* (2016) 'cAMP regulates the functional activity, coupling efficiency and structural organization of mammalian F O F 1 ATP synthase', *Biochimica et Biophysica Acta (BBA) - Bioenergetics*, 1857(4), pp. 350–358. doi: 10.1016/j.bbabio.2016.01.006.

Ercu, M. *et al.* (2020) 'Phosphodiesterase 3A and Arterial Hypertension', *Circulation*. Lippincott Williams and Wilkins, 142(2), pp. 133–149. doi: 10.1161/CIRCULATIONAHA.119.043061.

Franco, R., Bortner, C. D. and Cidlowski, J. A. (2006) 'Potential roles of electrogenic ion transport and plasma membrane depolarization in apoptosis', *Journal of Membrane Biology*, pp. 43–58. doi: 10.1007/s00232-005-0837-5.

Fromenty, B. (2020) 'Alteration of mitochondrial DNA homeostasis in drug-induced liver injury', *Food and Chemical Toxicology*. Elsevier Ltd, 135. doi: 10.1016/j.fct.2019.110916.

Gan, T. J. (2010) 'Diclofenac: an update on its mechanism of action and safety profile.', *Current Medical Research and Opinion*, 26(7), pp. 1715–1731. doi: 10.1185/03007995.2010.486301.

Gates, A. *et al.* (2009) 'cAMP-GEF cytoprotection by Src tyrosine kinase activation of phosphoinositide-3-kinase p110 β/α in rat hepatocytes', *American Journal of Physiology-Gastrointestinal and Liver Physiology*. American Physiological Society, 296(4), pp. G764–G774. doi: 10.1152/ajpgi.90622.2008.

Geng, Y. *et al.* (2020) 'Protective effect of metformin against palmitate-induced hepatic cell death.', *Biochimica et biophysica acta. Molecular basis of disease*. Elsevier B.V., 1866(3), p.

165621. doi: 10.1016/j.bbadis.2019.165621.

Gervin, K. *et al.* (2017) 'Long-term prenatal exposure to paracetamol is associated with DNA methylation differences in children diagnosed with ADHD', *Clinical Epigenetics*. BioMed Central Ltd., 9(1). doi: 10.1186/s13148-017-0376-9.

Gjertsen, B. T. *et al.* (1995) 'Novel (Rp)-cAMPS analogs as tools for inhibition of cAMP-kinase in cell culture. Basal cAMP-kinase activity modulates interleukin-1 beta action.', *The Journal of biological chemistry*. American Society for Biochemistry and Molecular Biology, 270(35), pp. 20599–607. doi: 10.1074/jbc.270.35.20599.

Hoivik, E. A. *et al.* (2013) 'DNA Methylation of Alternative Promoters Directs Tissue Specific Expression of Epac2 Isoforms', *PLoS ONE*, 8(7), p. 67925. doi: 10.1371/journal.pone.0067925.

Hong, G., Zhang, B. and Harbrecht, B. G. (2010) 'Cyclic AMP Inhibits IL-1β Plus IFNγ-Induced NF-κB Translocation in Hepatocytes by a PKA Independent Mechanism', *Journal of Surgical Research*. NIH Public Access, 159(1), pp. 565–571. doi: 10.1016/j.jss.2008.12.018.

Honrath, B. *et al.* (2017) 'SK2 channels regulate mitochondrial respiration and mitochondrial Ca2+ uptake', *Cell Death & Differentiation*, 24(5), pp. 761–773. doi: 10.1038/cdd.2017.2.

Insel, P. A. *et al.* (2012) 'Cyclic AMP is both a pro-apoptotic and anti-apoptotic second messenger', *Acta Physiologica (Oxford, England)*. NIH Public Access, 204(2), p. 277. doi: 10.1111/J.1748-1716.2011.02273.X.

Jakobsen, E., Lange, S. C. and Bak, L. K. (2019) 'Soluble adenylyl cyclase-mediated cAMP signaling and the putative role of PKA and EPAC in cerebral mitochondrial function', *Journal of Neuroscience Research*. John Wiley & Sons, Ltd, 97(8), pp. 1018–1038. doi: 10.1002/jnr.24477.

Johnston, A. *et al.* (2011) 'cAMP-guanine exchange factor protection from bile acid-induced hepatocyte apoptosis involves glycogen synthase kinase regulation of c-Jun NH_2-terminal kinase', *American Journal of Physiology-Gastrointestinal and Liver Physiology*, 301(2), pp. G385–G400. doi: 10.1152/ajpgi.00430.2010.

Lakics, V., Karran, E. H. and Boess, F. G. (2010) 'Quantitative comparison of phosphodiesterase mRNA distribution in human brain and peripheral tissues', *Neuropharmacology*, 59(6), pp. 367–374. doi: 10.1016/j.neuropharm.2010.05.004.

Lamb, H. M. (2020) 'Double agents of cell death: novel emerging functions of apoptotic

regulators', *FEBS Journal*, pp. 2647–2663. doi: 10.1111/febs.15308.

Lapeyre-Mestre, M., Grolleau, S. and Montastruc, J.-L. (2013) 'Adverse drug reactions associated with the use of NSAIDs: a case/noncase analysis of spontaneous reports from the French pharmacovigilance database 2002-2006', *Fundamental & Clinical Pharmacology*, 27(2), pp. 223–230. doi: 10.1111/j.1472-8206.2011.00991.x.

Laudette, M. *et al.* (2019) 'Identification of a pharmacological inhibitor of Epac1 that protects the heart against acute and chronic models of cardiac stress', *Cardiovascular Research*, 115(12), pp. 1766–1777. doi: 10.1093/cvr/cvz076.

Masubuchi, Y. (2002) 'Role of mitochondrial permeability transition in diclofenac-induced hepatocyte injury in rats', *Hepatology*, 35(3), pp. 544–551. doi: 10.1053/jhep.2002.31871.

Monterisi, S. *et al.* (2017) 'PDE2A2 regulates mitochondria morphology and apoptotic cell death via local modulation of cAMP/PKA signalling', *eLife*. eLife Sciences Publications Ltd, 6. doi: 10.7554/eLife.21374.

Moshage, H., Casini, A. and Lieber, C. S. (1990) 'Acetaldehyde selectively stimulates collagen production in cultured rat liver fat-storing cells but not in hepatocytes', *Hepatology*, 12(3), pp. 511–518. doi: 10.1002/hep.1840120311.

Ng, L. E. *et al.* (2006) 'Action of diclofenac on kidney mitochondria and cells', *Biochemical and Biophysical Research Communications*. Academic Press, 348(2), pp. 494–500. doi: 10.1016/J.BBRC.2006.07.089.

Papa, S. *et al.* (1999) 'cAMP-dependent protein kinase and phosphoproteins in mammalian mitochondria. An extension of the cAMP-mediated intracellular signal transduction', *FEBS Letters*, 444(2–3), pp. 245–249. doi: 10.1016/S0014-5793(99)00070-8.

Perry, S. W. *et al.* (2011) 'Mitochondrial membrane potential probes and the proton gradient: a practical usage guide', *Biotechniques*, 50(2), pp. 98–115. doi: 10.2144/000113610.

Rehmann, H. (2013) 'Epac-Inhibitors: Facts and Artefacts'. *Scientific Reports*, 3. doi: 10.1038/srep03032.

Rizzuto, R. *et al.* (1998) 'Close contacts with the endoplasmic reticulum as determinants of mitochondrial Ca2+ responses', *Science*. American Association for the Advancement of Science, 280(5370), pp. 1763–1766. doi: 10.1126/science.280.5370.1763.

Rodríguez-Antona, C. *et al.* (2002) 'Cytochrome P450 expression in human hepatocytes and hepatoma cell lines: Molecular mechanisms that determine lower expression in cultured

cells', *Xenobiotica*. Taylor & Francis, 32(6), pp. 505–520. doi: 10.1080/00498250210128675.

Santos-Alves, E. *et al.* (2014) 'Exercise mitigates diclofenac-induced liver mitochondrial dysfunction', *European Journal of Clinical Investigation*, 44(7), pp. 668–677. doi: 10.1111/eci.12285.

Sanuki, Y. *et al.* (2017) 'A rapid mitochondrial toxicity assay utilizing rapidly changing cell energy metabolism', *The Journal of Toxicological Sciences*, 42(3), pp. 349–358. doi: 10.2131/jts.42.349.

Schippers, M. *et al.* (2017) 'Upregulation of Epac-1 in Hepatic Stellate Cells by Prostaglandin E 2 in Liver Fibrosis Is Associated with Reduced Fibrogenesis s', *THE JOURNAL OF PHARMACOLOGY AND EXPERIMENTAL THERAPEUTICS J Pharmacol Exp Ther*, 363, pp. 126–135. doi: 10.1124/jpet.117.241646.

Schmidt, M., Dekker, F. J. and Maarsingh, H. (2013) 'Exchange Protein Directly Activated by cAMP (epac): A Multidomain cAMP Mediator in the Regulation of Diverse Biological Functions'. doi: 10.1124/pr.110.003707.

Schoemaker, M. H. *et al.* (2002) 'Cytokine regulation of pro- and anti-apoptotic genes in rat hepatocytes: NF-kappaB-regulated inhibitor of apoptosis protein 2 (cIAP2) prevents apoptosis.', *Journal of hepatology*, 36(6), pp. 742–50. doi: 10.1016/s0168-8278(02)00063-6.

Seitz, S. and Boelsterli, U. A. (1998) 'Diclofenac acyl glucuronide, a major biliary metabolite, is directly involved in small intestinal injury in rats', *Gastroenterology*, 115(6), pp. 1476–1482. doi: 10.1016/S0016-5085(98)70026-5.

Sinclair, E. M. *et al.* (2008) 'Glucagon Receptor Signaling Is Essential for Control of Murine Hepatocyte Survival', *Gastroenterology*. W.B. Saunders, 135(6), pp. 2096–2106. doi: 10.1053/J.GASTRO.2008.07.075.

Sivertsen Åsrud, K. *et al.* (2019) 'Mice depleted for Exchange Proteins Directly Activated by cAMP (Epac) exhibit irregular liver regeneration in response to partial hepatectomy', *Scientific Reports*. Nature Publishing Group, 9(1). doi: 10.1038/s41598-019-50219-8.

Syed, M., Skonberg, C. and Hansen, S. H. (2016) 'Mitochondrial toxicity of diclofenac and its metabolites via inhibition of oxidative phosphorylation (ATP synthesis) in rat liver mitochondria: Possible role in drug induced liver injury (DILI)', *Toxicology in Vitro*. Pergamon, 31, pp. 93–102. doi: 10.1016/J.TIV.2015.11.020.

Szanda, G. *et al.* (2018) 'Mitochondrial cAMP exerts positive feedback on mitochondrial Ca2+ uptake via the recruitment of Epac1', *Journal of Cell Science*. Company of Biologists Ltd, 131(10). doi: 10.1242/jcs.215178.

Ueno, H. *et al.* (2001) 'Characterization of the Gene EPAC2: Structure, Chromosomal Localization, Tissue Expression, and Identification of the Liver-Specific Isoform', *Genomics*, 78(1–2), pp. 91–98. doi: 10.1006/geno.2001.6641.

Valsecchi, F., Konrad, C. and Manfredi, G. (2014) 'Role of soluble adenylyl cyclase in mitochondria', *Biochimica et Biophysica Acta - Molecular Basis of Disease*. Elsevier, pp. 2555–2560. doi: 10.1016/j.bbadis.2014.05.035.

Wang, Z. *et al.* (2016) 'A cardiac mitochondrial cAMP signaling pathway regulates calcium accumulation, permeability transition and cell death', *Cell Death and Disease*. Nature Publishing Group, 7(4). doi: 10.1038/cddis.2016.106.

Wiggins, S. V. *et al.* (2018) 'Pharmacological modulation of the CO 2 /HCO 3− /pH-, calcium-, and ATP-sensing soluble adenylyl cyclase', *Pharmacology and Therapeutics*. Elsevier Inc., pp. 173–186. doi: 10.1016/j.pharmthera.2018.05.008.

Yang, Y. *et al.* (2016) 'EPAC activation inhibits acetaldehyde-induced activation and proliferation of hepatic stellate cell via Rap1', *Canadian Journal of Physiology and Pharmacology*, 94(5), pp. 498–507. doi: 10.1139/cjpp-2015-0437.

Yang, Z. *et al.* (2017) 'Epac2-Rap1 Signaling Regulates Reactive Oxygen Species Production and Susceptibility to Cardiac Arrhythmias',*Antioxidants and redox signaling*,27(3). doi: 10.1089/ars.2015.6485.

Zuo, H. *et al.* (2019) 'Function of cAMP scaffolds in obstructive lung disease: Focus on epithelial-to-mesenchymal transition and oxidative stress', *British Journal of Pharmacology*. John Wiley and Sons Inc., pp. 2402–2415. doi: 10.1111/bph.14605.

Molecular Pharmacology Fast Forward. Published on February 11, 2021 as DOI: 10.1124/molpharm.120.000217
This article has not been copyedited and formatted. The final version may differ from this version.

Conflict of Interest statement and funding

The authors declare that they have no conflict of interest with other people or organizations during the preparation of this work.

Fabio Aguilar Mora was supported by a personal grant from Conacyt (CVU614256)

Martina Schmidt was supported by a grant from the Deutsche Forschungsgemeinschaft (IRTG1874 DIAMICOM-SP2) and an unrestricted grant from Novartis (50199468)

5. Figure legends

Figure 1. Elevation of cAMP prevents DF-induced caspase-3 activation in primary rat hepatocytes. Panel A and B show the fold induction of caspase-3 activity vs control. Cells were incubated with diclofenac 400 µmol/L in the presence and absence of forskolin 10 µmol/L (panel A) or IBMX 100 µmol/L (panel B) added 30 min before diclofenac exposure. The use of forskolin and IBMX alone do not cause significant induction of caspase 3 activity. Diclofenac and/or elevation of cAMP levels do not induce significant necrotic cell death as determined by Sytox green staining (panel C). Scale bar 250µm. Two-tailed Mann-Whitney u test was used to determine statistical significance (n=6). Data are presented as the mean ± standard deviation of the mean (SD) ($P \leq 0.00005$ = ****, $P \leq 0.0005$ = ***, $P \leq 0.005$ = **, ns = $P \geq 0.05$).

Figure 2. The PKA inhibitor RP-8CPT-cAMPS (RP) only partially reverses the protective effect of forskolin (panel A) but not IBMX (panel B) against DF-induced apoptosis in primary rat hepatocytes. PKA inhibitor alone does not cause cell death. Cells were incubated with diclofenac (DF, 400 µmol/L, 12 hr) with and without RP-8CPT-cAMPS (100 µmol/L, 12 hr) added 20 min before forskolin (F, 10 µmol/L) or IBMX (I, 100 µmol/L) added 30 min before diclofenac exposure. Two-tailed Mann-Whitney u test was used to determine statistical significance (n=6). Data are presented as the mean ± standard deviation of the mean (SD) ($P \leq 0.05$ = *, ns = $P \geq 0.05$).

Figure 3. Both EPAC inhibitor CE3F4 and ESI-05 reverses the protective effect of forskolin (panel A and C) and IBMX (panel B and D) against DF-induced apoptosis in primary rat

hepatocytes. EPAC inhibitors alone do not significantly increase caspase 3 activity. Cells were incubated with diclofenac (DF, 400 µmol/L, 12 hr) with and without ESI-05 (ES, 15 µmol/L) or CEFA4 (CE, 10 µmol/L) in the presence or absence of forskolin (, 10 µmol/L) or IBMX (100 µmol/L) added 30 min before diclofenac exposure. Two-tailed Mann-Whitney u test was used to determine statistical significance (n=6). Data are presented as the mean ± standard deviation of the mean (SD) (P≤0.00005 = ****, P≤ 0.0005 = ***, P≤0.005 = **, ns = P≥ 0.05).

Figure 4. Relative mRNA expression of EPAC1 and EPAC2 in different liver cell types. Panel A: EPAC1 mRNA is high in liver sinusoidal endothelial cells (LSECs) and intermediate in activated stellate cells (stellate cells activated), but low in (primary) hepatocytes and Kupffer cells. Panel B: EPAC1 expression, LSECs data set was omitted to emphasize the expression of EPAC1 in (primary) rat hepatocytes and Kupffer cells. Panel C: EPAC2 mRNA expression is high in hepatocytes, intermediate in LSECs and activated stellate cells but absent in Kupffer cells. Panel D: mRNA expression of EPAC2 isoforms in primary rat hepatocytes. EPAC2C mRNA and EPAC2B mRNA are expressed in hepatocytes, whereas EPAC2A mRNA is not detected in hepatocytes.

Figure 5. Immunofluorescence and Western blot analysis of EPACs. Panel A: Immunofluorescence analysis shows expression of EPAC1 and EPAC2 in primary cultures of rat hepatocytes. EPAC1 shows a punctate-like staining pattern. Nuclei are stained blue with DAPI. Negative controls are without primary antibody. Scale bar 10µm. Panel B: EPAC1 protein is expressed in rat hepatocytes mitochondria and whole cell lysate. 'WCL' is whole cell lysate. 'Total' is total cell lysate, 'cytosol' is the cytosolic fraction while 'mito' is the

mitochondria fraction. EPAC1-HA overexpressed in HEK 293 cells was used as a molecular weight control for EPAC1. β-actin was used as a loading control. EPAC1 set represent n = 8 from at least 3 biological replicates (independent rat isolations). Panel C: EPAC2 isoforms (2B and 2C) are expressed in rat hepatocyte mitochondria and whole cell lysate. 'WCL' is whole cell lysate. 'Total' is total cell lysate, 'cytosol' is the cytosolic fraction while 'mito' is the mitochondria fraction. Human hippocampus, rat heart and human EPAC2A and EPAC2B, overexpressed in HEK 293 cells, were used as controls. β-actin was used as a loading control while Tim23 was used as a control for mitochondria samples and EPAC2 set represent n= 3 biological replicates (independent rat hepatocyte isolations).

Figure 6. Elevation of cAMP does not prevent ATP depletion caused by DF in primary rat hepatocytes. The panels show the percentage of luminescence (RLU) normalized to the control condition. Cells were incubated with diclofenac (DF, 400 µmol/L, 2 and 4 hr) in the presence and absence of forskolin (, 10µmol/L, 2 and 4 hr) or IBMX (100µmol/, 2 and 4 hr) added 30 min before diclofenac exposure. Panel A shows ATP levels 2 hours after DF exposure; panel B shows ATP levels 4 hours after DF exposure. Two-tailed Mann-Whitney u test was used to determine statistical significance (n=9). Data are presented as the mean ± standard deviation of the mean (SD) $P \leq 0.00005$ = ****, ns = $P \geq 0.05$).

Figure 7. Elevation of cAMP prevents early mitochondrial membrane potential depolarization induced by diclofenac in primary hepatocytes. Cells were incubated with diclofenac (DF, 400 µmol/L, 2 hr) with and without forskolin 10µmol/L or IBMX 100µmol/L added 30 min before diclofenac exposure. Panel A shows JC-10 staining for the different conditions. Scale bar 250µm. Panels B and C show the quantitative representation of the

fluorescence intensity red/green ratio of the JC-10 staining. Quantification of the fluorescence intensity ratio red/green was calculated by comparing the IntDen of the red and green channels, avoiding the quantification of dead cells and normalizing the data to the mean IntDen of the control condition. Two-tailed Mann-Whitney u test was used to determine statistical significance (n=6). Data are presented as the mean ± standard deviation of the mean (SD) ($P \leq 0.0005$ = ***, $P \leq 0.005$ = **, $P \leq 0.05$ = *, ns = $P \geq 0.05$).

Figure 8. EPAC1 inhibition (CE3F4; panel A,C) but not EPAC2 inhibition (ESI-05; panel A,C) slightly but significantly reduce the protective effect of forskolin against DF-induced mitochondrial membrane potential depolarization. EPAC inhibitors alone do not cause significant alterations to the mitochondrial membrane potential (panel A,B,C). Panel A: show fluorescence intensity (ratio red/green). Scale bar 250µm. Cells were incubated with diclofenac (DF) 400 µmol/L, 2 hr with and without ESI-05(ES) 15 µmol/L or CE3F4 (CE) 10 µmol/L added 30 min before forskolin 10µmol/L added 30 min before diclofenac exposure. Panels B and C show quantification of the fluorescence intensity ratio red/green which was calculated by comparing the IntDen of the red and green channels avoiding the quantification of dead cells and normalizing the data to the mean IntDen of the control condition. Two-tailed Mann-Whitney u test was used to determine statistical significance (n=6). Data are presented as the mean ± standard deviation of the mean (SD) ($P \leq 0.05$ = *, ns = $P \geq 0.05$).

Figure 9. The EPAC2 inhibitor ESI-05 (panel A,B) but not the EPAC1 inhibitor CE3F4 (CE) (panel A,C) abolishes the protective effect of IBMX against DF-induced mitochondrial membrane potential depolarization in primary hepatocytes. EPAC inhibitors alone do not cause significant alterations in the mitochondrial membrane potential. The figures show

fluorescence intensity (ratio red/green). Cells were incubated with diclofenac (DF) 400 µmol/L, 2 hr with and without ESI-05(ES) 15 µmol/L or CE3F4 (CE) 10 µmol/L added 30 min before IBMX 100µmol/L added 30 min before diclofenac exposure. Quantification of the fluorescence intensity ratio red/green was calculated by comparing the IntDen of the red and green channels avoiding the quantification of dead cells and normalizing the data to the mean IntDen of the control condition. Two-tailed Mann-Whitney u test was used to determine statistical significance (n=6). Data are presented as the mean ± standard deviation of the mean (SD) ($P \leq 0.05$ = *, ns = $P \geq 0.05$).

Figure 10. Proposed mechanism of the protective effect of cAMP-EPAC against diclofenac-induced toxicity in rat hepatocytes. Diclofenac toxic metabolites are derived mainly from phase I metabolism in the endoplasmic reticulum (ER). Phase I metabolism is driven by the cytochrome P450 family (CYP2C9, CYP3A4 and CYP2C8 in humans or CYP3A1, CYP2C6 and CYP2C11 in rats). As a result, 4'-hydroxydiclofenac (4-OH), 5-hydroxydiclofenac (5-OH) and unidentified mono- and dihydroxylated metabolites are formed (Arnaiz *et al.*, 1995; Boelsterli, 2003). When GSH and/or NAD(P)H are depleted, diclofenac metabolites accumulate and cause ER stress, inducing C/EBP homologous protein (CHOP). As a consequence, the IP_3R_1 calcium ion release channel is activated, inducing a mitochondrial overload of Ca^{2+} through sites of close contact called mitochondria-associated ER membranes (MAMs), causing a potential difference between the cytosol and the inner mitochondrial membrane potential ($\Delta\Psi m$) (Rizzuto *et al.*, 1998). Sustained high levels of Ca^{2+} in the mitochondria trigger the release of cytochrome c, Apaf-1 and ATP. These molecules bind to procaspase 9, leading to apoptosome formation and activation of caspase 9, which activates caspase 3, followed by apoptosis (Lamb, 2020). Apoptosis induced by diclofenac is prevented by the use of cAMP elevating agents (forskolin and IBMX). The

Molecular Pharmacology Fast Forward. Published on February 11, 2021 as DOI: 10.1124/molpharm.120.000217
This article has not been copyedited and formatted. The final version may differ from this version.

cAMP elevating agents promote cAMP accumulation via direct activation of pmAC or the inhibition of PDEs. cAMP accumulation is compartmentalized and activate via either EPAC1 (primarily localized in the mitochondria) or both EPAC2 (localized in mitohcondria and cytosol). Depicted is a potential (mitochondrial) AC-cAMP-EPAC1 and PDE-cAMP-EPAC2 domain. EPAC activation will then prevent $\Delta\Psi m$ depolarization, preventing the activation of caspase 3 and apoptotic cell death. For further details, see text.

FIGURE 1

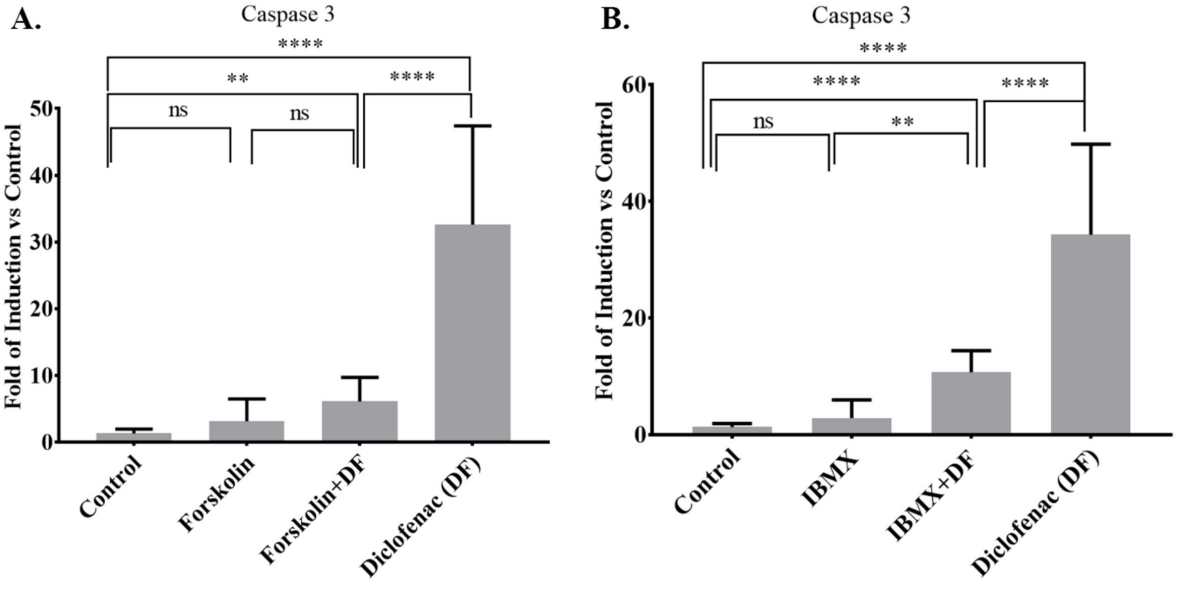
A.
Caspase 3
****
**
****
ns
ns
Fold of Induction vs Control
50
40
30
20
10
0
Control
Forskolin
Forskolin+DF
Diclofenac (DF)
B.
Caspase 3
****
****
****
ns
**
Fold of Induction vs Control
60
40
20
0
Control
IBMX
IBMX+DF
Diclofenac (DF)

C.

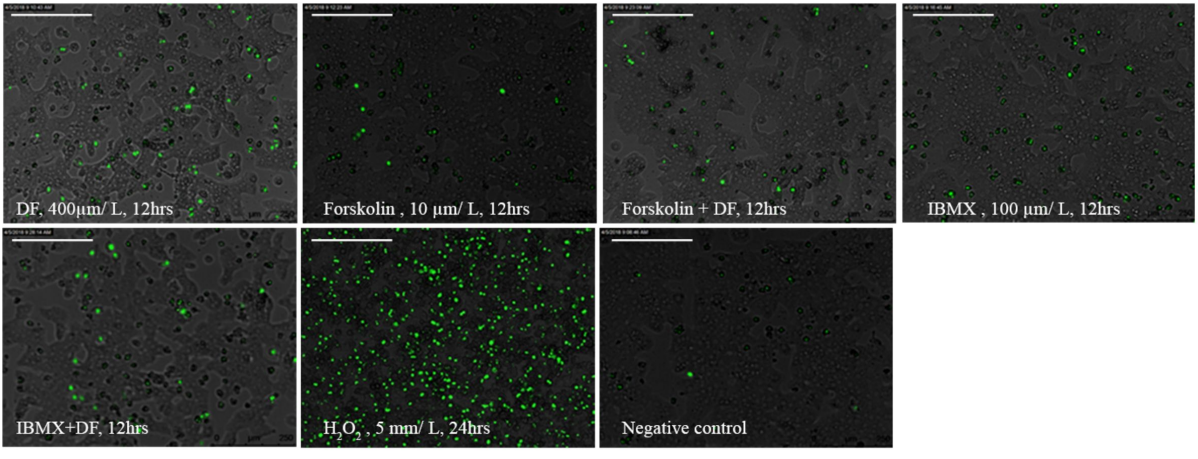
DF, 400µm/ L, 12hrs
Forskolin , 10 µm/ L, 12hrs
Forskolin + DF, 12hrs
IBMX , 100 µm/ L, 12hrs
IBMX+DF, 12hrs
H_2O_2 , 5 mm/ L, 24hrs
Negative control

FIGURE 2

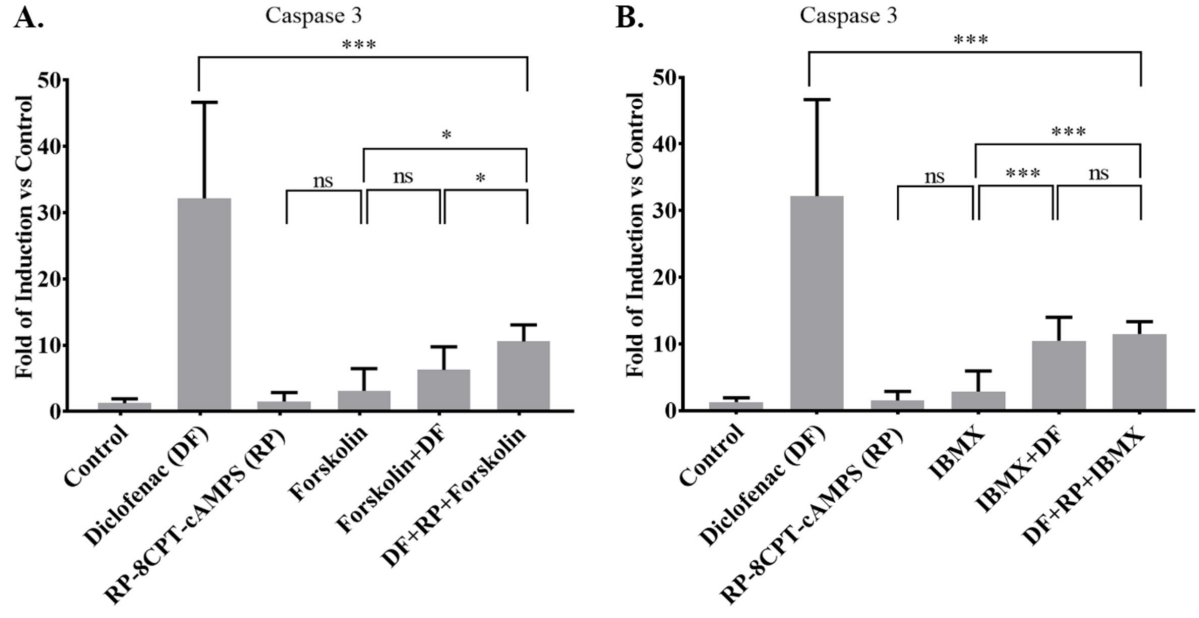
A.
Caspase 3
Fold of Induction vs Control
50
40
30
20
10
0
***
*
ns
ns
*
Control
Diclofenac (DF)
RP-8CPT-cAMPS (RP)
Forskolin
Forskolin+DF
DF+RP+Forskolin
B.
Caspase 3
Fold of Induction vs Control
50
40
30
20
10
0
***
***
ns
***
ns
Control
Diclofenac (DF)
RP-8CPT-cAMPS (RP)
IBMX
IBMX+DF
DF+RP+IBMX

FIGURE 3

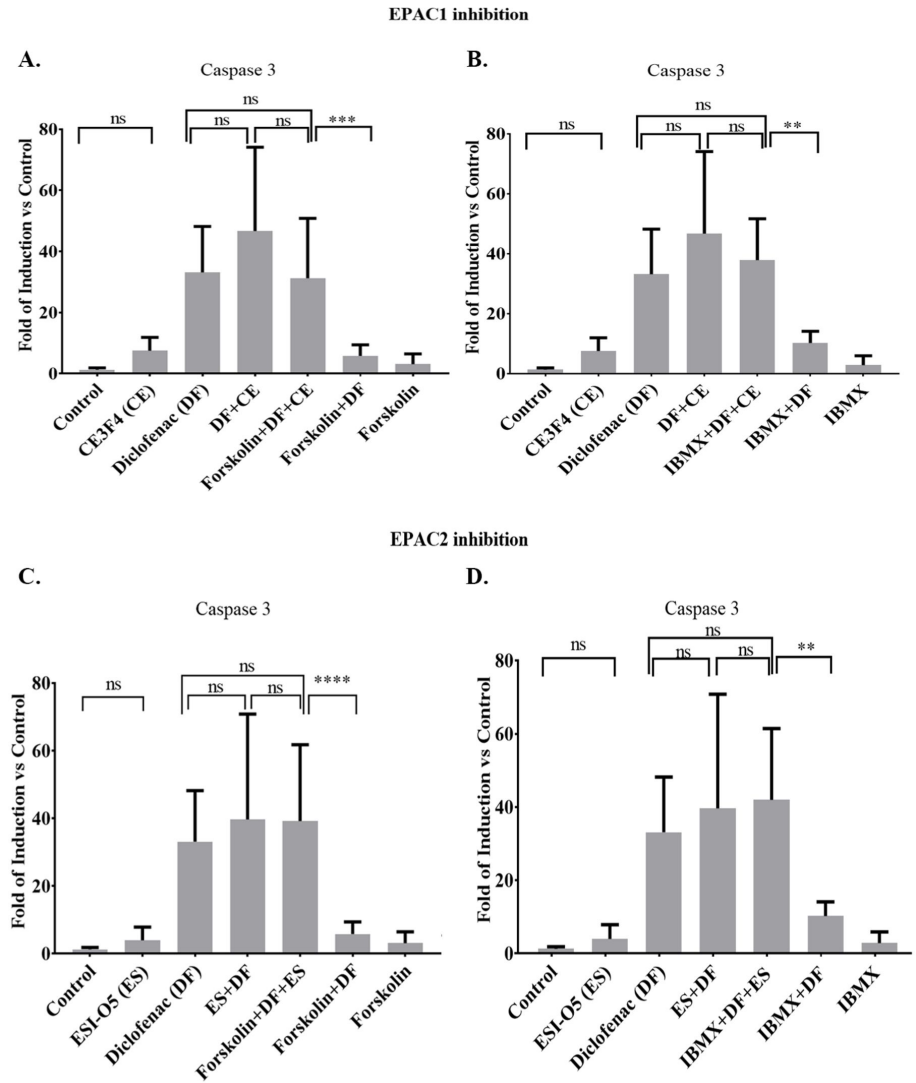
EPAC1 inhibition
A.
Caspase 3
Fold of Induction vs Control
ns
ns
ns
ns
***
Control
CE3F4 (CE)
Diclofenac (DF)
DF+CE
Forskolin+DF+CE
Forskolin+DF
Forskolin
B.
Caspase 3
Fold of Induction vs Control
ns
ns
ns
ns
**
Control
CE3F4 (CE)
Diclofenac (DF)
DF+CE
IBMX+DF+CE
IBMX+DF
IBMX
EPAC2 inhibition
C.
Caspase 3
Fold of Induction vs Control
ns
ns
ns
ns
****
Control
ESI-05 (ES)
Diclofenac (DF)
ES+DF
Forskolin+DF+ES
Forskolin+DF
Forskolin
D.
Caspase 3
Fold of Induction vs Control
ns
ns
ns
ns
**
Control
ESI-05 (ES)
Diclofenac (DF)
ES+DF
IBMX+DF+ES
IBMX+DF
IBMX

FIGURE 4

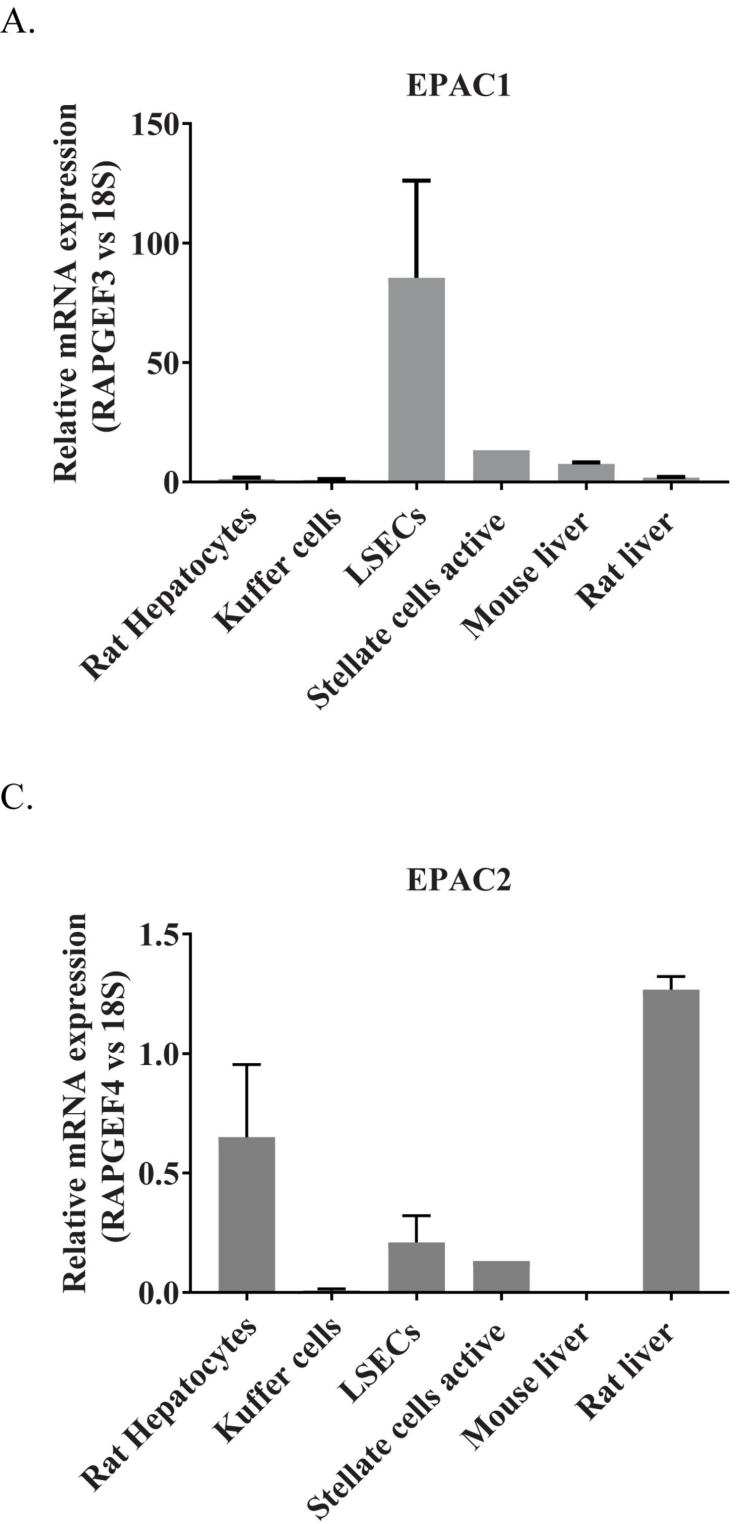

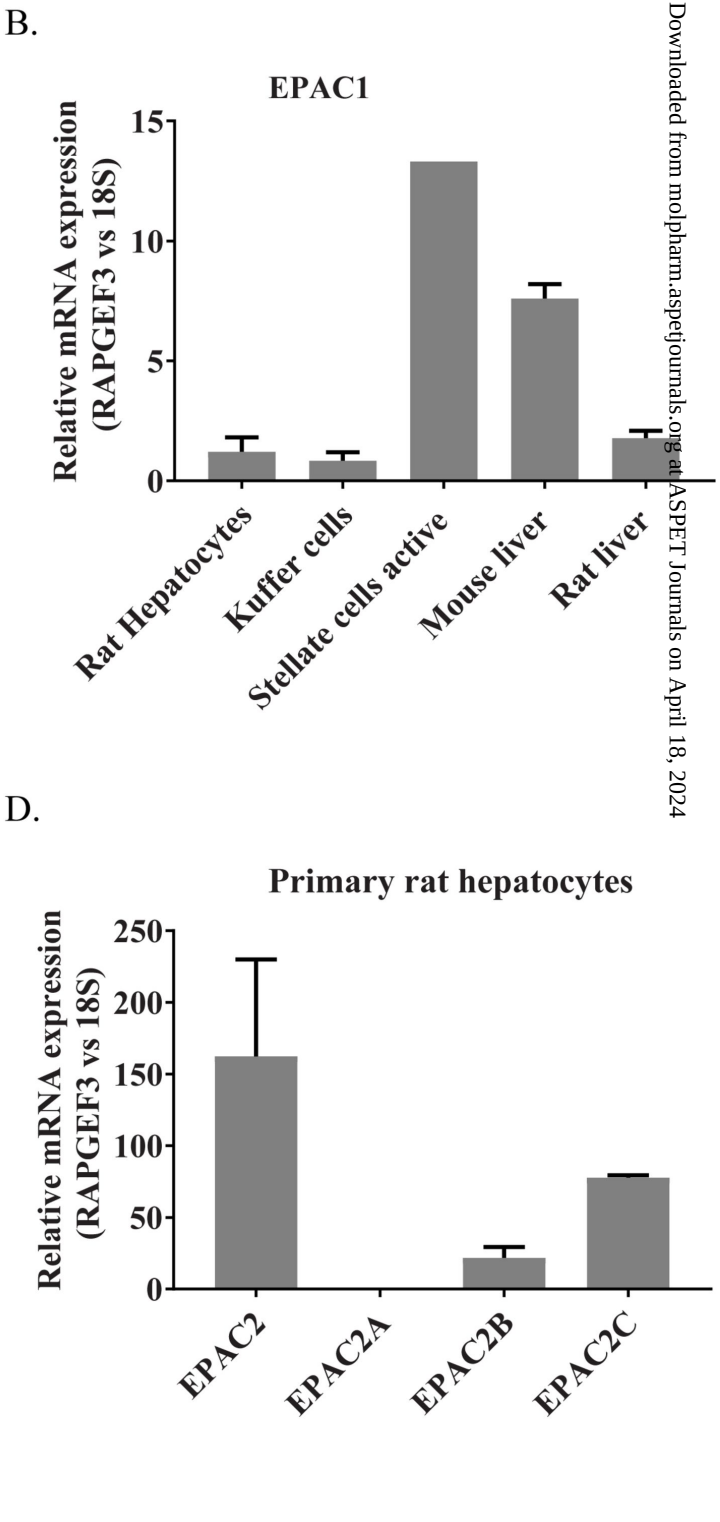

FIGURE 5

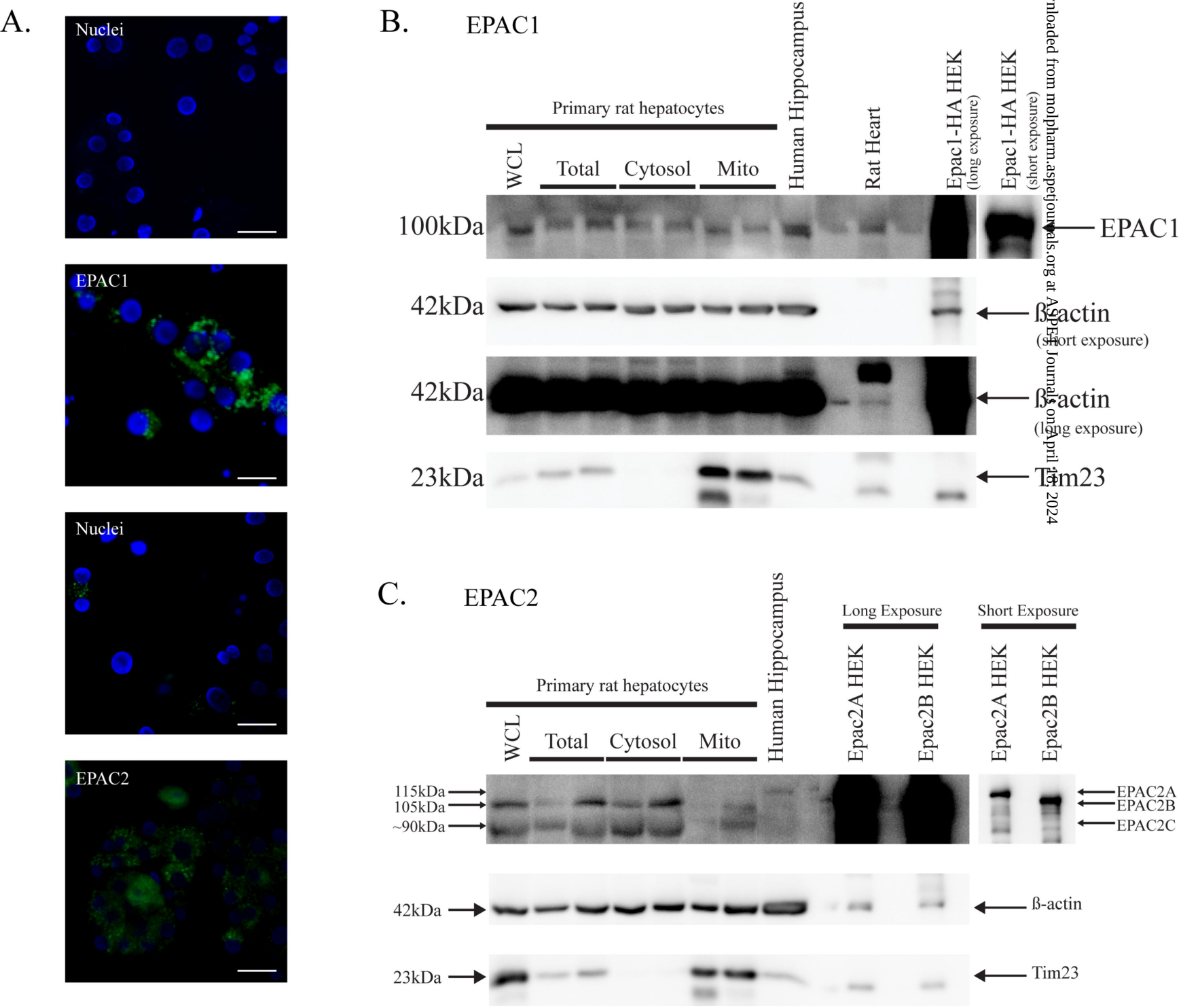

FIGURE 6

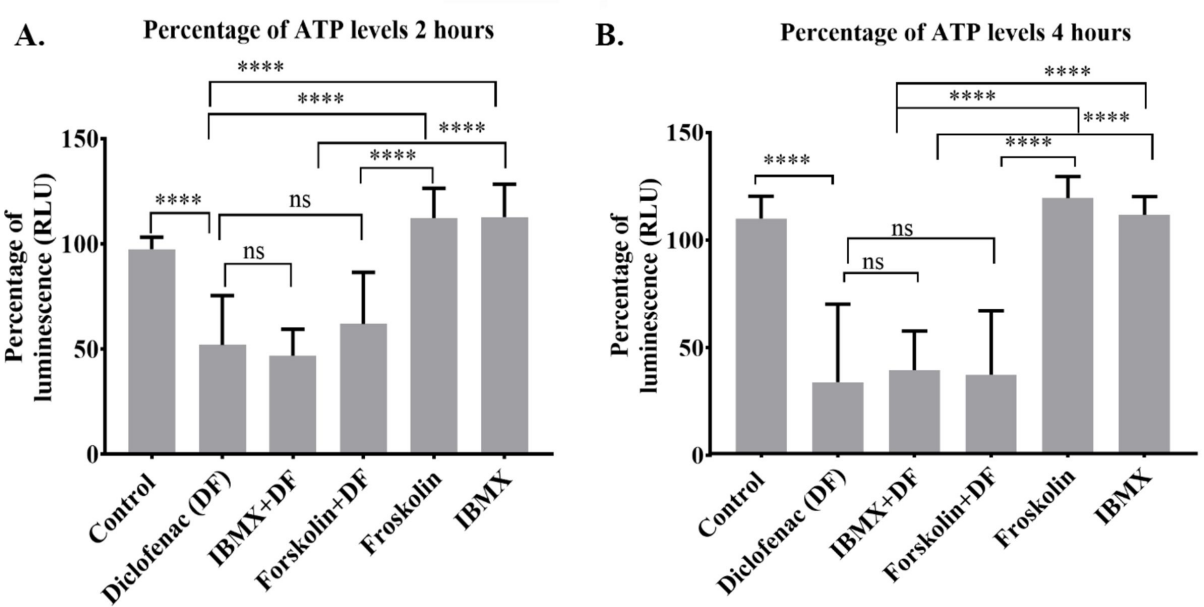
A.
Percentage of ATP levels 2 hours
Percentage of luminescence (RLU)
150
100
50
0
****
****
****
****
****
ns
ns
Control
Diclofenac (DF)
IBMX+DF
Forskolin+DF
Froskolin
IBMX
B.
Percentage of ATP levels 4 hours
Percentage of luminescence (RLU)
150
100
50
0
****
****
****
****
****
ns
ns
Control
Diclofenac (DF)
IBMX+DF
Forskolin+DF
Froskolin
IBMX

FIGURE 7

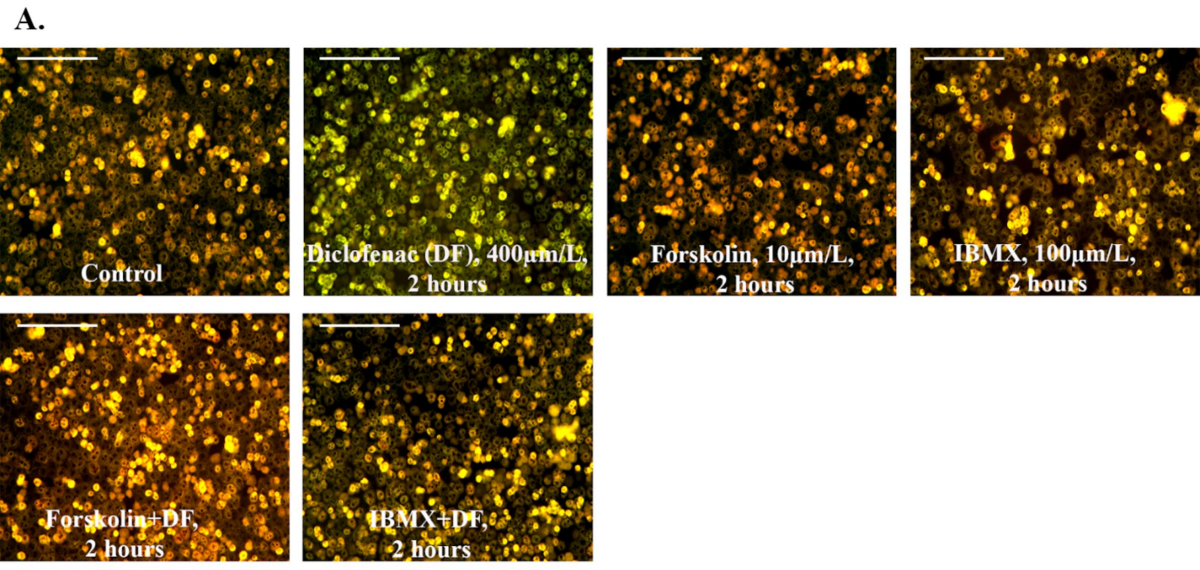
A.
Control
Diclofenac (DF), 400µm/L, 2 hours
Forskolin, 10µm/L, 2 hours
IBMX, 100µm/L, 2 hours
Forskolin+DF, 2 hours
IBMX+DF, 2 hours

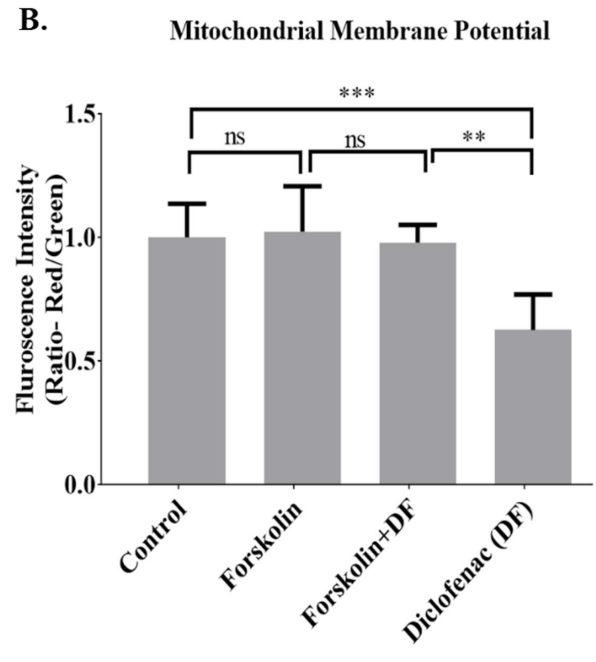
B.
Mitochondrial Membrane Potential
Fluroscence Intensity (Ratio- Red/Green)
1.5
1.0
0.5
0.0
***
ns
ns
**
Control
Forskolin
Forskolin+DF
Diclofenac (DF)

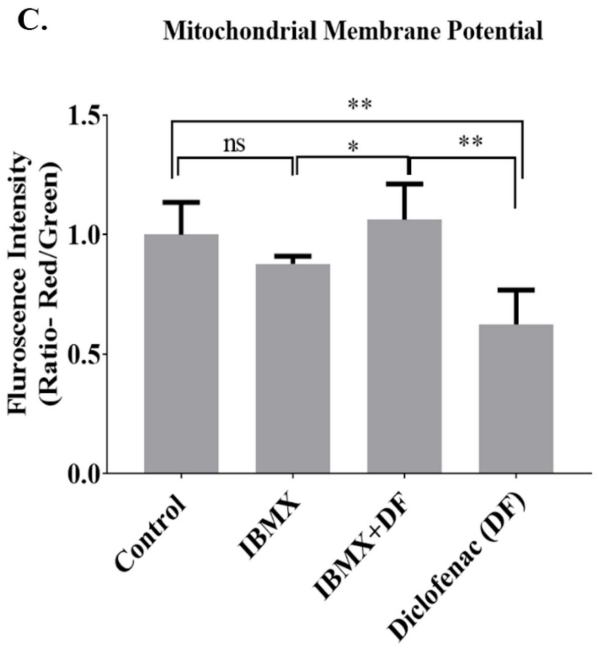
C.
Mitochondrial Membrane Potential
Fluroscence Intensity (Ratio- Red/Green)
1.5
1.0
0.5
0.0
**
ns
*
**
Control
IBMX
IBMX+DF
Diclofenac (DF)

FIGURE 8

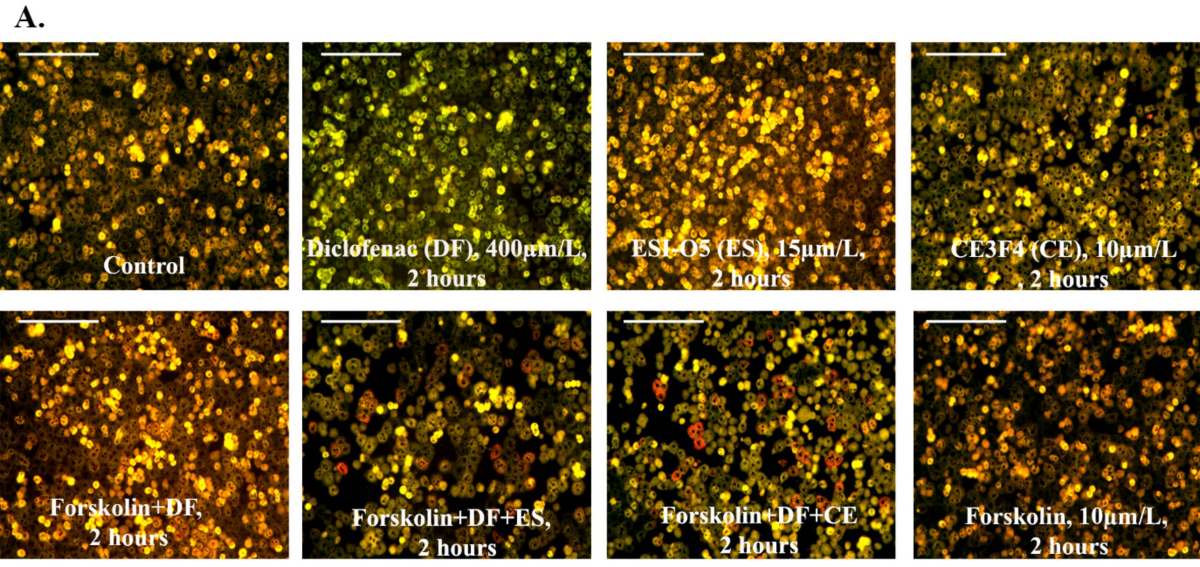
A.
Control
Diclofenac (DF), 400µm/L, 2 hours
ESI-O5 (ES), 15µm/L, 2 hours
CE3F4 (CE), 10µm/L, 2 hours
Forskolin+DF, 2 hours
Forskolin+DF+ES, 2 hours
Forskolin+DF+CE 2 hours
Forskolin, 10µm/L, 2 hours

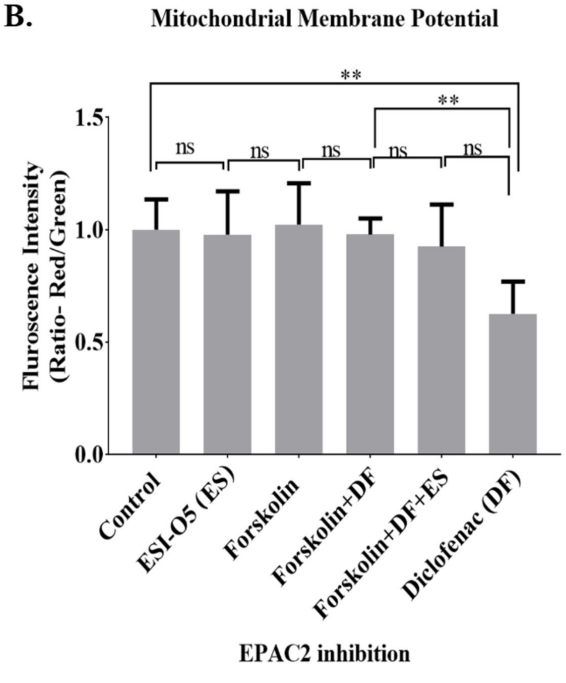
B.
Mitochondrial Membrane Potential
Fluroscence Intensity (Ratio- Red/Green)
1.5
1.0
0.5
0.0
**
**
ns
ns
ns
ns
ns
Control
ESI-O5 (ES)
Forskolin
Forskolin+DF
Forskolin+DF+ES
Diclofenac (DF)
EPAC2 inhibition

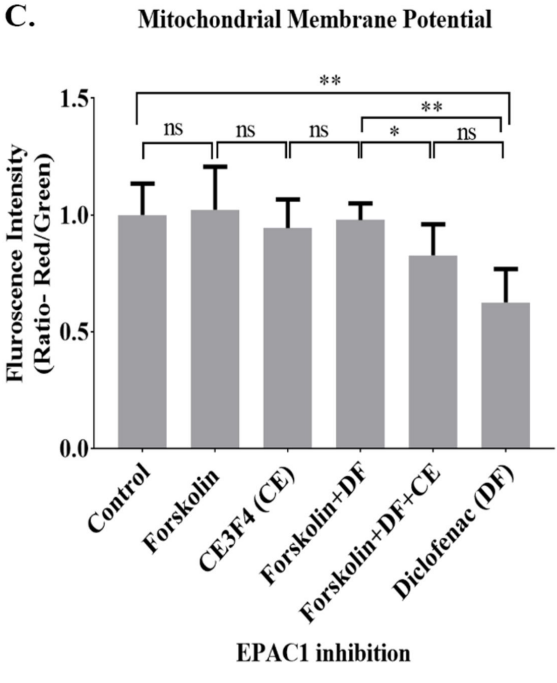
C.
Mitochondrial Membrane Potential
Fluroscence Intensity (Ratio- Red/Green)
1.5
1.0
0.5
0.0
**
**
*
ns
ns
ns
ns
ns
Control
Forskolin
CE3F4 (CE)
Forskolin+DF
Forskolin+DF+CE
Diclofenac (DF)
EPAC1 inhibition

FIGURE 9

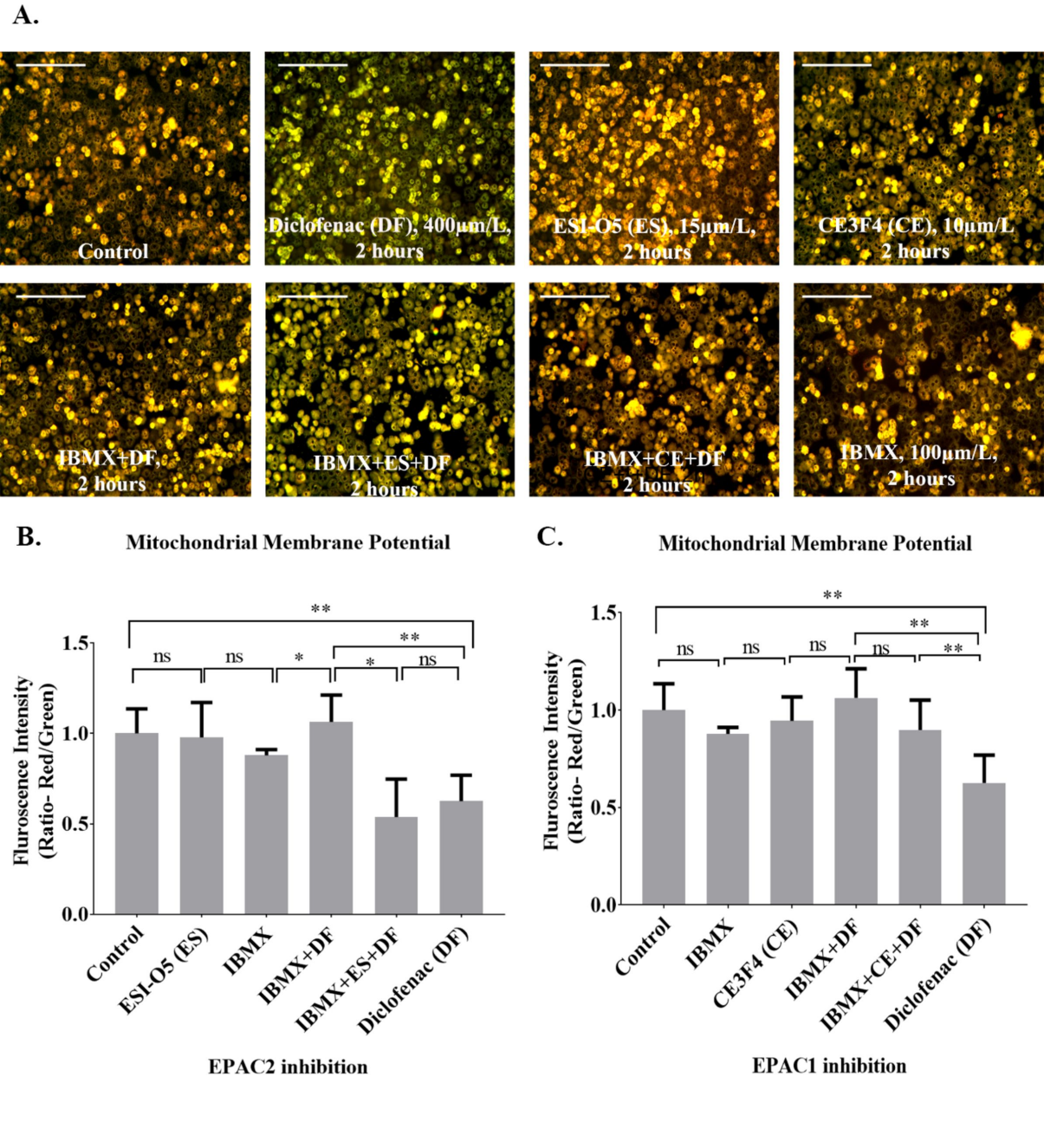
A.
Control
Diclofenac (DF), 400µm/L, 2 hours
ESI-O5 (ES), 15µm/L, 2 hours
CE3F4 (CE), 10µm/L 2 hours
IBMX+DF, 2 hours
IBMX+ES+DF 2 hours
IBMX+CE+DF 2 hours
IBMX, 100µm/L, 2 hours
B.
Mitochondrial Membrane Potential
Fluroscence Intensity (Ratio- Red/Green)
1.5
1.0
0.5
0.0
**
**
*
*
ns
ns
ns
Control
ESI-O5 (ES)
IBMX
IBMX+DF
IBMX+ES+DF
Diclofenac (DF)
EPAC2 inhibition
C.
Mitochondrial Membrane Potential
Fluroscence Intensity (Ratio- Red/Green)
1.5
1.0
0.5
0.0
**
**
**
ns
ns
ns
ns
Control
IBMX
CE3F4 (CE)
IBMX+DF
IBMX+CE+DF
Diclofenac (DF)
EPAC1 inhibition

FIGURE 10

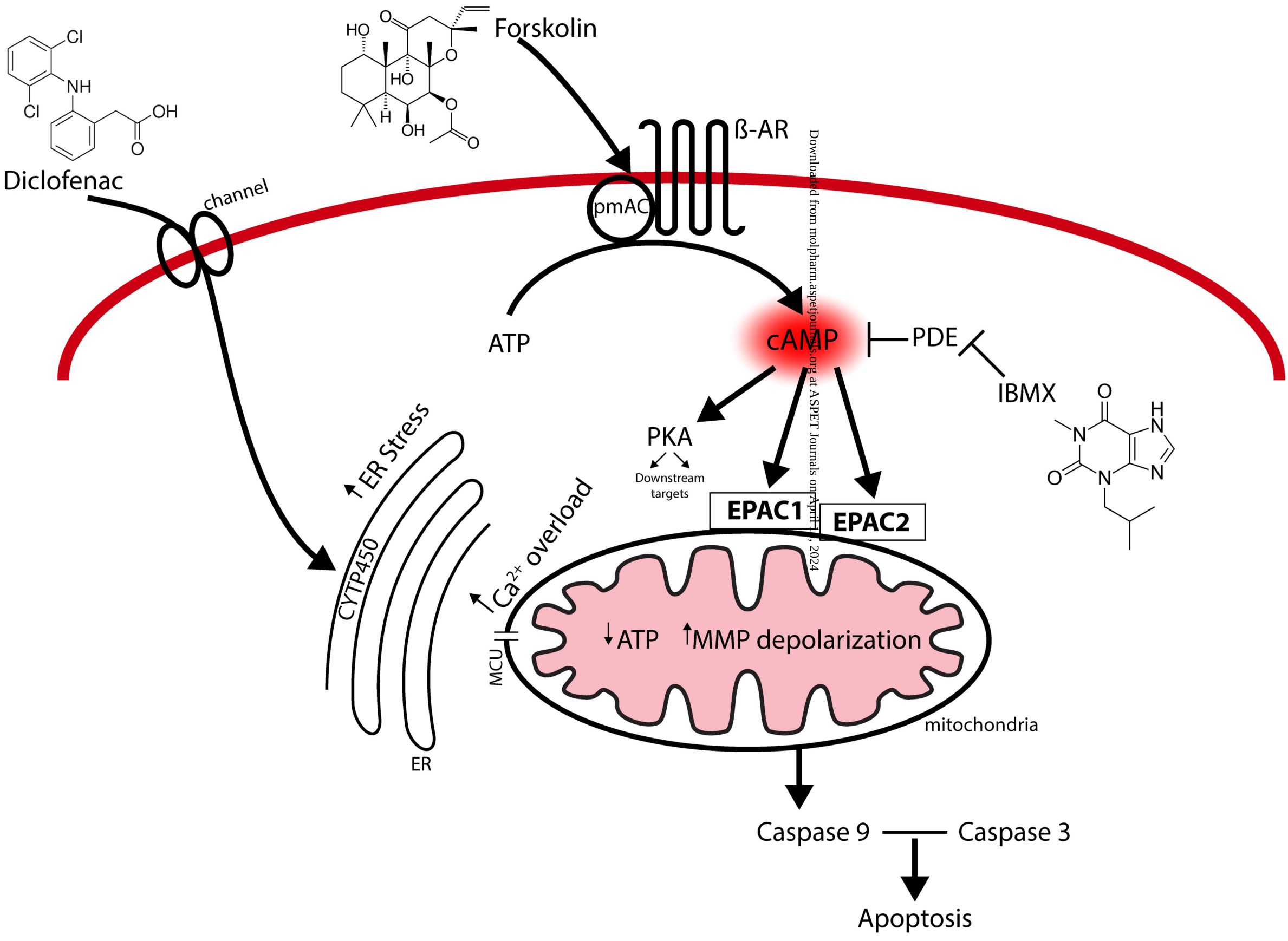

Fabio Alejandro Aguilar Mora, Nshunge Musheshe, Asmaa Oun, Manon Buist-Homan, Frank Lezoualc'h, Xiaodong Cheng, Martina Schmidt, Han Moshage

Elevated cAMP protects against diclofenac-induced toxicity in primary rat hepatocytes: a protective effect mediated by EPACs

MOLPHARM-AR-2020-000217

Molecular Pharmacology

SUPPLEMENTARY FIGURE 1

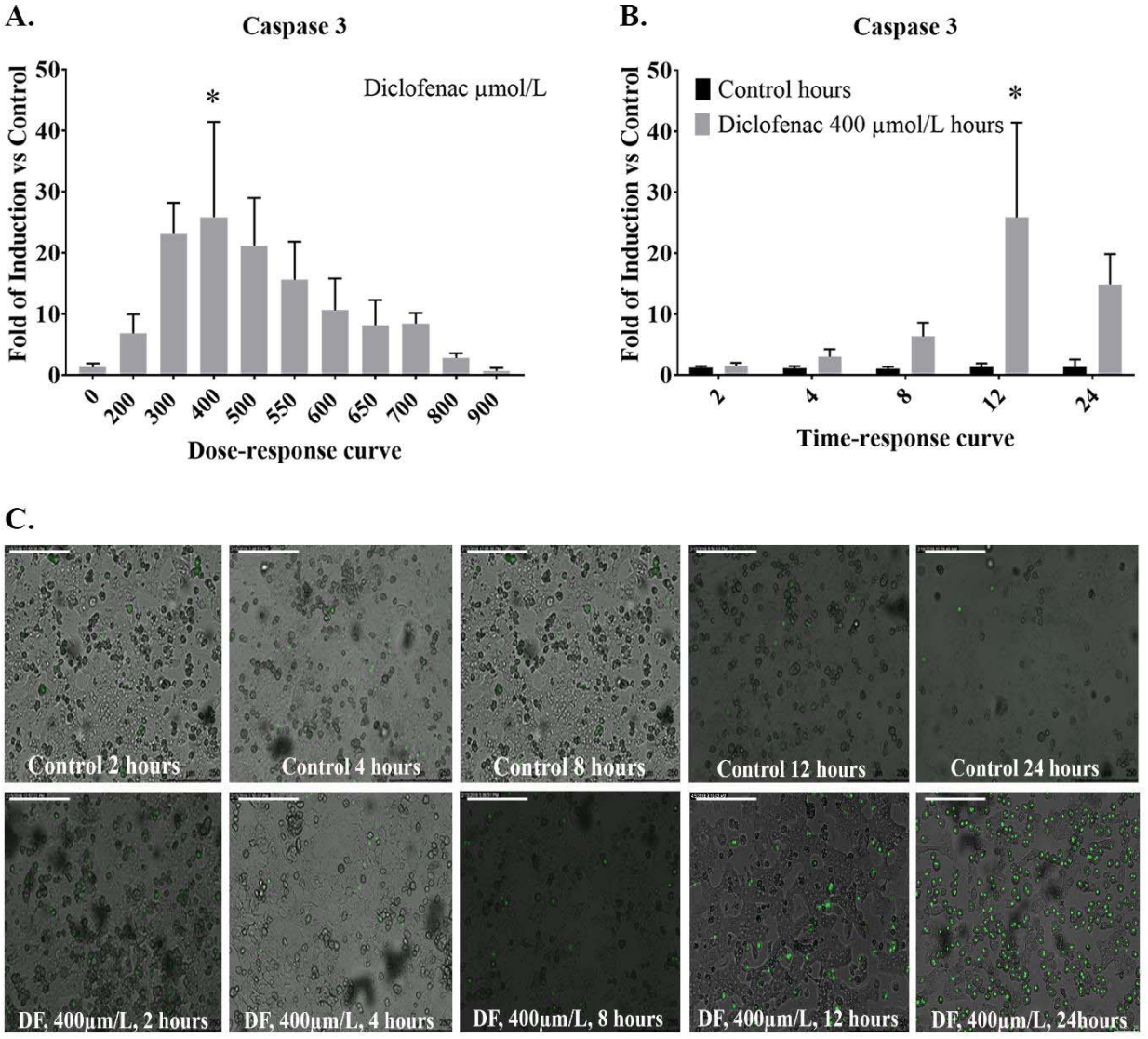

Supplementary Figure 1. Toxicity of diclofenac (DF). Dose/time-response curve of caspase-3 activity in primary rat hepatocytes. Panel A: Cells were incubated with diclofenac, 0- 900 µmol/L for 12 hours, and caspase-3 activity was measured to determine apoptotic cell death. Panel B: Cells were incubated with diclofenac at 400 µmol/L for 2h-24h with or without diclofenac and caspase-3 activity was measured to determine apoptotic cell death. Panel C: Hepatocytes were treated with diclofenac at 400 µmol/L for 24 hours. Necrotic cell death was assessed using Sytox green staining. Scale bar 250µm. Data are presented as the mean ± standard deviation of the mean (SD) ($P \leq 0.00005$ = ****, $P \leq 0.0005$ = ***, $P \leq 0.005$ = **, $P \leq 0.05$ = *, ns = $P \geq 0.05$). Two-tailed Mann-Whitney u test was used to determine statistical significance (n=6).

SUPPLEMENTARY FIGURE 2

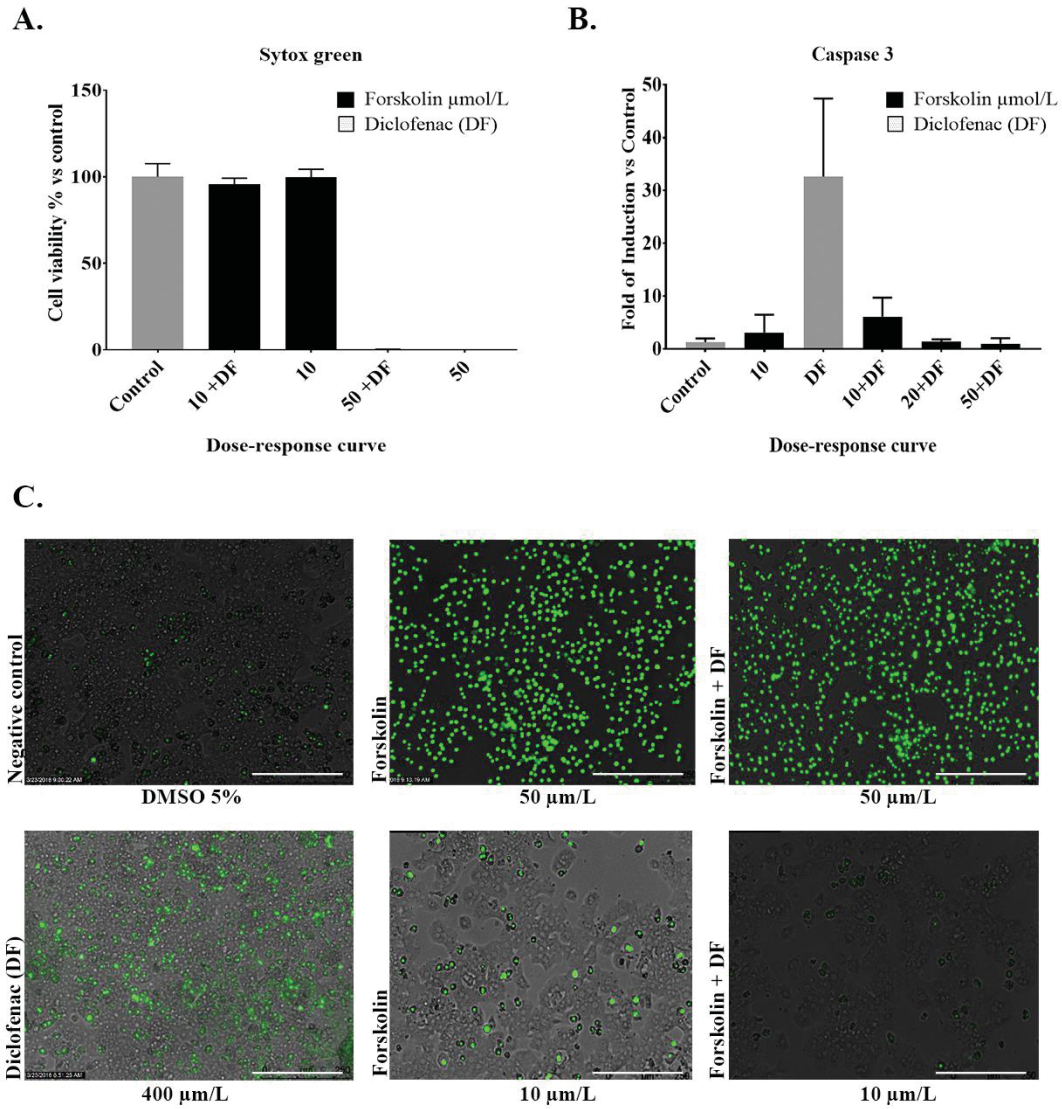

Supplementary Figure 2. Dose-response curve to determine forskolin toxicity in primary rat hepatocytes. Panel A: Necrotic cell death determined by Sytox green staining. Cells were incubated with diclofenac 400 µmol/L for 12 hours in the presence of forskolin 10-50 µmol/L added 30 min before diclofenac exposure. Panel B: Apoptotic cell death determined by caspase-3 activity assay. Hepatocytes were treated with diclofenac at 400 µmol/L in the presence of forskolin 10-50 µmol/L for 12 hours. Panel C: Visual representation of necrotic cell death assessed using Sytox green staining and used for quantification depicted in panel A. Scale bar 250µm. Data are presented as the mean ± standard deviation of the mean (SD) (n=6).

SUPPLEMENTARY FIGURE 3

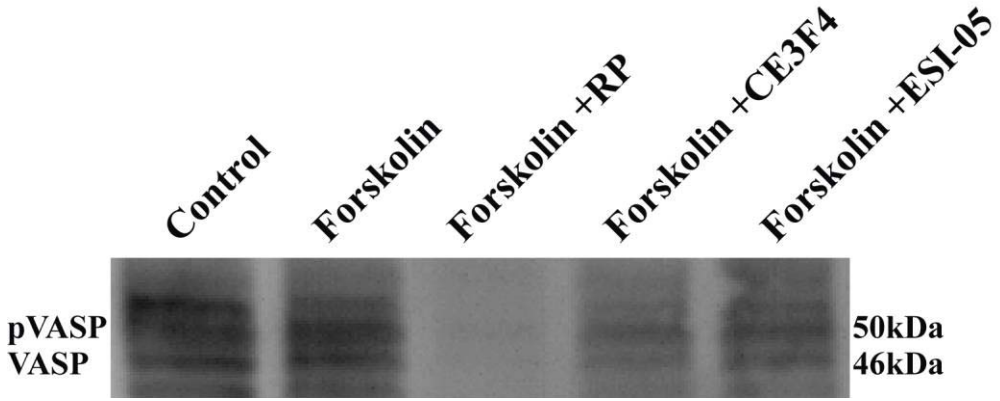

Supplementary Figure 3. Western blot analysis of VASP phosphorylation in primary rat hepatocytes treated with forskolin. To inhibit PKA, RP (RP-8CPT-cAMP was used, the EPAC1 inhibitor CE3F4 and the EPAC2 inhibitor ESI-05 served as controls.

SUPPLMENTARY FIGURE 4

A.

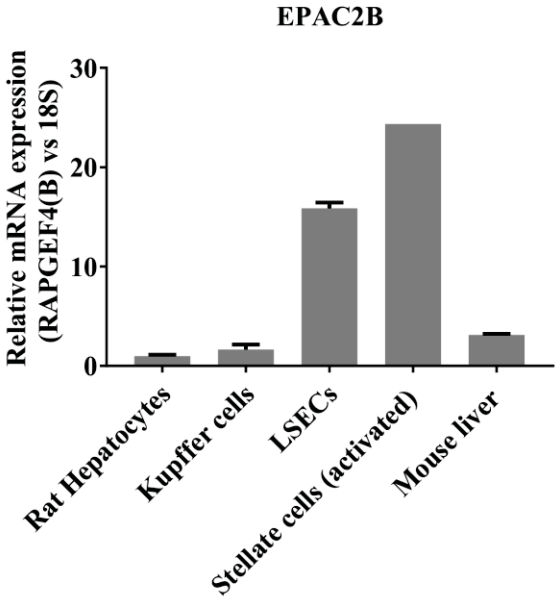

B.

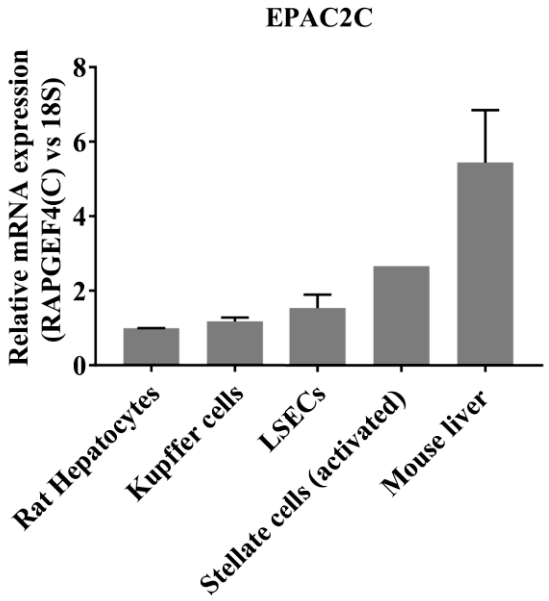

C.

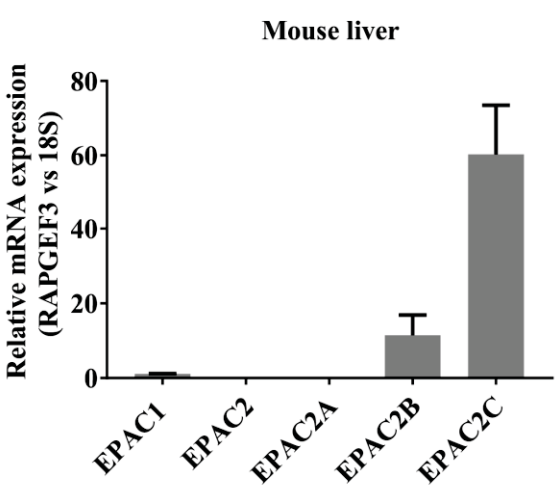

Supplementary Figure 4. Relative mRNA expression of EPAC2 isoforms in different rat liver cell types. Panel A shows that EPAC2B is expressed mainly in LSECs and activated stellate cells. Panel B shows that EPAC2C is expressed in all liver cell types. Panel C shows the relative expression of EPAC2 isoforms in mouse liver. Data are presented as the mean ± standard deviation of the mean (SD) (n=6), stellate cell-active data set is presented as the mean ± standard deviation of the mean (SD) (n=3).

Supplementary Table 1 Overview of primers used for qRT-PCR					
Target region	**Direction**	**Sequence (5'–3')**	**PCR Size (bp)**	**Target exon/UTR**	**Species**
EPAC2 A1/2	F	CACGCGGCTGAAAGGAGTTAA	561	Exon 2	Mus musculus
	R	ATCATGTGGGGAGCTCGAGAGA		Exon 8	
EPAC2 B	F	TGGCTGCTTACTGGATGTCTGAGAA	274	5' UTR of exon 1b	Mus musculus
	R	ATCATGTGGGGAGCTCGAGAGA			
EPAC2 C	F	GCCTCCATGTTTCCCGCAG	228	5' UTR of exon 10	Mus musculus
	R	GTCATCCACAGTCCTCTGGCCA		Exon 11	
Universal EPAC1		Determined by the provider, TaqMan® (Thermo Fisher Scientific, Sunol Blvd, Pleasanton, CA) catalog number Rn00572463_m1			Rat
Universal EPAC2		Determined by the provider and TaqMan® (Thermo Fisher Scientific, Sunol Blvd, Pleasanton, CA) catalog number Rn01514839_m1			Rat
18S	F	CGG CTA CCA CAT CCA AGG A		Exon 1	Mus musculus
	R	CCA ATT ACA GGG CCT CGA AA			
	Probe	CGCGCAAATTACCCACTCCCGA			

Supplementary Table 2: Quantification of % cell viability using Sytox green staining as a way to discriminate between necrotic and non-necrotic cells due to its cell membrane stability in primary rat hepatocytes (Conde de la Rosa *et al.*, 2006). Diclofenac results are in line with other researchers suggesting that diclofenac toxicity is mainly apoptotic (Aithal and Day, 2007).

Quantification of % cell viability using Sytox green staining				
	Median (Interquartile range)	**% Differences vs Negative control**	**P Value**	**N**
Negative Control	101,8 (94,95 - 106,7)			
Forskolin 50 µmol/L 12 hours	0 (0.3 -0.8)	102%	<0,0001	8
Forskolin 50 µmol/L +DF 12 hours	0 (0.4 - 0.9)	100%	<0,0001	8
Forskolin10 µmol/L +DF 12 hours	95,72 (93,85-97,98)	6%	0,1153	8
Forskolin10 µmol/L 12 hours	100,1 (96,15-103,6)	2%	0,6239	8
Diclofenac (DF) 400 µmol/L 24 hours	40,96 (9,22-56,94)	60%	<0,0001	8
Diclofenac (DF) 400 µmol/L 12 hours	95,85 (87,78 - 98,1)	6%	0,0819	12
Diclofenac (DF) 400 µmol/L 8 hours	90.01 (88.26- 93,01)	11%	0.004	8
Diclofenac (DF) 400 µmol/L 4 hours	99.17 (95.53- 103)	3%	0.62	8
Diclofenac (DF) 400 µmol/L 2 hours	100.8 (93.47- 104.8)	1%	0.79	8
ESIO5 15 µmol/L 12 hours	96,32 (95,03-97,61)	5%	0,3531	8
CE3F4 10 µmol/L 12 hours	94,69 (93,79-96,01)	7%	0,045	8
IBMX 100 µmol/+DF 12 hours	100,7 (98,5-102,1)	1%	0,9671	8
IBMX 100 µmol/L 12 hours	99,94 (95,07-106,7)	2%	0,9699	8
H2O2 5mmol/L 24 hours Positive Control	0 (0.1 - 0.8)			